van Hinsbergen, D. J. J., Steinberger, B., Doubrovine, P., Gassmöller, R. (2011): Acceleration and deceleration of India-Asia convergence since the Cretaceous: roles of mantle plumes and continental collision. - Journal of Geophysical Research, 116, B06101

DOI: 10.1029/2010JB008051

Acceleration and deceleration of India-Asia convergence since the Cretaceous: Roles of mantle plumes and continental collision

Douwe J. J. van Hinsbergen,[1,2] Bernhard Steinberger,[1,2,3] Pavel V. Doubrovine,[1,2] and René Gassmöller[3,4]

Received 20 October 2010; revised 20 January 2011; accepted 3 March 2011; published 2 June 2011.

[1] A strong 50–35 Ma decrease in India-Asia convergence is generally ascribed to continent-continent collision. However, a convergence rate increase of similar magnitude occurred between ~65–50 Ma. An earlier increase occurred at ~90 Ma. Both episodes of accelerated convergence followed upon arrival of a mantle plume below and emplacement of a large igneous province (LIP) on the Indian plate. We here first confirm these convergence rate trends, reassessing the Indo-Atlantic plate circuits. Then, using two different numerical models, we assess whether plume head arrival and its lateral asthenospheric flow may explain the plate velocity increases and whether decreased plume flux and increasing continent-plume distance may explain deceleration, even without continental collision. The results show that plume head arrival can indeed lead to absolute Indian plate motion accelerations on the order of several cm/yr, followed by decelerations on timescales similar to the reconstructed fluctuations. The 90 Ma increase could potentially be explained as response to the Morondova mantle plume alone. The 65–50 Ma convergence rate increase, however, is larger than can be explained by plume head spreading alone. We concur with previous hypotheses that plume-induced weakening of the Indian continental lithosphere-asthenosphere coupling and an increased slab pull and ridge push efficiency are the most likely explanations for the large convergence rate increase. The post-50 Ma decrease is best explained by orogeny-related increased trench resistivity, decreased slab pull due to continental subduction, and possibly restrengthening of lithosphere-asthenosphere coupling upon plume demise.

Citation: van Hinsbergen, D. J. J., B. Steinberger, P. V. Doubrovine, and R. Gassmöller (2011), Acceleration and deceleration of India-Asia convergence since the Cretaceous: Roles of mantle plumes and continental collision, *J. Geophys. Res.*, *116*, B06101, doi:10.1029/2010JB008051.

1. Introduction

[2] The India-Asia continental collision is among the most spectacular tectonic events that occurred in Cenozoic time and is crucial in shaping our understanding of the influence of continent-continent collision on orogeny, plate motion and plate boundary evolution. In addition, collision formed the Himalayas and the Tibetan plateau, which may have had profound effects on global climate [*Dupont-Nivet et al.*, 2007; *Royden et al.*, 2008].

[3] To analyze the effects of continental collision and subduction, and its influences on topography and climate, it is essential to estimate the age of collision. Most authors prefer an age around 55–50 Ma for collision between the Tethyan Himalayas (the structurally highest, paleogeographically northernmost remnants of continental Greater India) and the southernmost continental terrane of Tibet for reasons reviewed in section 2. One of these arguments, however, is derived from global plate circuits (and apparent polar wander paths constructed using those), which shows that the India-Asia convergence rate dramatically decreased from ~16 cm/yr around 50 Ma to ~5 cm/yr around 35 Ma [*Molnar and Tapponnier*, 1975; *Klootwijk*, 1984; *Patriat and Achache*, 1984; *Besse and Courtillot*, 2002; *Torsvik et al.*, 2008; *Molnar and Stock*, 2009; *Copley et al.*, 2010]. This rapid relative plate convergence decrease is normally suggested to be causally related to, and hence is evidence for a ~55–50 Ma onset of the India-Asia collision.

[4] When inspecting the India-Asia convergence curves based on the Indo-Atlantic plate circuit [e.g., *Torsvik et al.*,

[1]Physics of Geological Processes, University of Oslo, Oslo, Norway.
[2]Center for Advanced Study, Norwegian Academy of Science and Letters, Oslo, Norway.
[3]Helmholtz Centre Potsdam, German Research Centre for Geosciences, Potsdam, Germany.
[4]Institute for Geosciences, Friedrich Schiller University, Jena, Germany.

0148-0227/11/2010JB008051

2008] since the middle Cretaceous, not only the 50–35 Ma deceleration, (and a smaller second one around 25–20 Ma [*Molnar and Stock*, 2009]) become apparent, but also an equally impressive acceleration since ~66 Ma from 8 to 16 cm/yr, on a similar timescale as the slowdown [e.g., *Patriat and Achache*, 1984; *Molnar and Stock*, 2009; *Copley et al.*, 2010]. Moreover, a preceding, less dramatic but equally clear, India-Asia plate convergence rate increase occurred at ~90 Ma. Before ascribing the deceleration of the India-Asia relative plate motion to continental subduction of Greater India (collision), it is essential to analyze the potential dynamic causes for the accelerations. For instance, if the process that is responsible for the acceleration ceases to exist, this may induce a slowdown even without collision.

[5] The rapid increases in India-Asia plate convergence rates around 90 and 65 Ma are associated with relocation of oceanic spreading centers, and are both in space and time associated with the arrival of a mantle plume, and the emplacement of a large igneous province (LIP).

[6] Around 90 Ma, coincident with the emplacement of the 91–84 Ma Morondova LIP by the arrival of Marion plume, seafloor spreading started between Madagascar and India/Seychelles [*Torsvik et al.*, 2000; *Bardintzeff et al.*, 2010]. Following the emplacement of the Deccan LIP by the Reunion plume at around 65 Ma, an eastward jump of the spreading ridge between India and Madagascar transferred the Seychelles microcontinent from the Indian plate to Africa [*Hofmann et al.*, 2000; *Collier et al.*, 2008; *Ganerød et al.*, 2011].

[7] Also earlier breakup phases of east Gondwana follow this pattern, with ~130 Ma spreading between India and Antarctica being associated with the Kerguelen LIP [*Gaina et al.*, 2007], and Jurassic separation of Madagascar and Antarctica from Africa following emplacement of the Karoo LIP [*Jourdan et al.*, 2007; *Eagles and Konig*, 2008; see also *Gnos et al.*, 1997].

[8] A causal relationship between mantle plume arrival below continental lithosphere and rifting and opening of oceanic basins has long been suggested [*Burke and Dewey*, 1973; *White and McKenzie*, 1989; *Hill*, 1991; *Courtillot et al.*, 1999].

[9] In addition, *Gurnis and Torsvik* [1994] argued that arrival of hot mantle plumes below a plate may both increase the potential gravitational energy of a plate, as well as impose lateral mantle flow, which may induce an increase in plate velocity, especially when it contains a thick continental lithospheric root. Alternatively, *Kumar et al.* [2007] suggested that the multiple plumes that affected the evolution of the Indian continent thinned its lithosphere and weakened the lithosphere-asthenosphere coupling. This would lead to an increased effectiveness of ridge push and slab pull, even if these forces remain constant, which would result in acceleration of India-Asia convergence. Both effects may have led to the anomalously high India-Asia plate convergence rates around 55–50 Ma.

[10] Plume head arrivals are relatively short-lived features, and if plume head arrival accelerates a plate [*Gurnis and Torsvik*, 1994], its disappearance (i.e., the decrease of the plume-related heat flux and cooling of partially molten mantle due to volcanism, conduction and hydrothermal circulation) may thus decelerate the plate, even without collision. However, if plumes thin the continental root and weaken the lithosphere-asthenosphere coupling [*Kumar et al.*, 2007], plate motion deceleration is more likely to result from the combined effects of absolute decrease of slab pull due to continental subduction, increased resistance at the convergent plate boundary due to orogeny, and perhaps restrenghtening of lithosphere-asthenosphere coupling due to migration of the plate or the continental lithosphere away from the plume. In this case, the timing of slowdown may be used to infer continental collision.

[11] In this paper, we therefore aim to test (1) whether plume head arrival is indeed likely to generate accelerations of India-Asian convergence; (2) whether the total relative plate motion rate, especially since 65 Ma, can be entirely ascribed to plume head spreading; and (3) whether the disappearance of a plume head can generate the 50–35 Ma India-Asia deceleration, or whether an additional slowing factor (e.g., related to continental subduction) needs to be invoked. To this end, we reassess the relative India-Asia plate motion rates by combining relative plate motions estimated using marine geophysical data from the Atlantic and Indian oceans. Then, we show results of numerically simulated changes in plate motion induced by the arrival of a mantle plume. The maximum effect is estimated with two different numerical models (one without and one with lateral viscosity variations) where the plume arrives exactly at the plate boundary. For the first model, we also assess the effect of changing plate geometry, using a realistic plate reconstruction. Finally, we discuss the influences of mantle plumes and continental collision on India-Asia relative plate motion rates.

[12] The numerical modeling results are by definition expressed in terms of "absolute" motion, i.e., motion of the Indian plate relative to the mantle. When comparing with observed plate motions, it appears therefore most appropriate to also consider plate motions in an "absolute" reference frame. Here we use the Indo-Atlantic moving hot spot reference frame of *O'Neill et al.* [2005], i.e., plate motions are defined relative to hot spots, taking the observed geometry and age progression of hot spot tracks into account, but also considering that hot spots have moved relative to each other [*Molnar and Atwater*, 1973]. The motion of hot spots is computed by *O'Neill et al.* [2005] from a numerical model of plume conduits embedded in large-scale mantle flow. On the other hand, however, we consider for observed plate motion changes also the motion of the Indian plate relative to Eurasia, because this is what is reflected in the geological history. Furthermore, relative plate motions within the African hemisphere are known with considerably less uncertainty than absolute motions, and by looking at relative motions we hence avoid possible artifacts which may be due to the choice of the uncertain absolute reference frame. This treatment may at first sight seem inconsistent. However, we will also show that the changes in motion which we are concerned about in this paper appear in a very similar fashion in both the absolute and relative motion history, because, during the time period of interest, Eurasia has moved little with respect to the mantle compared to India.

2. Indian Plate Evolution Since 130 Ma: Passive and Active Margins, and the Size of Greater India

[13] The establishment of the Indian plate by separation from Gondwana occurred around 130–120 Ma, upon initi-

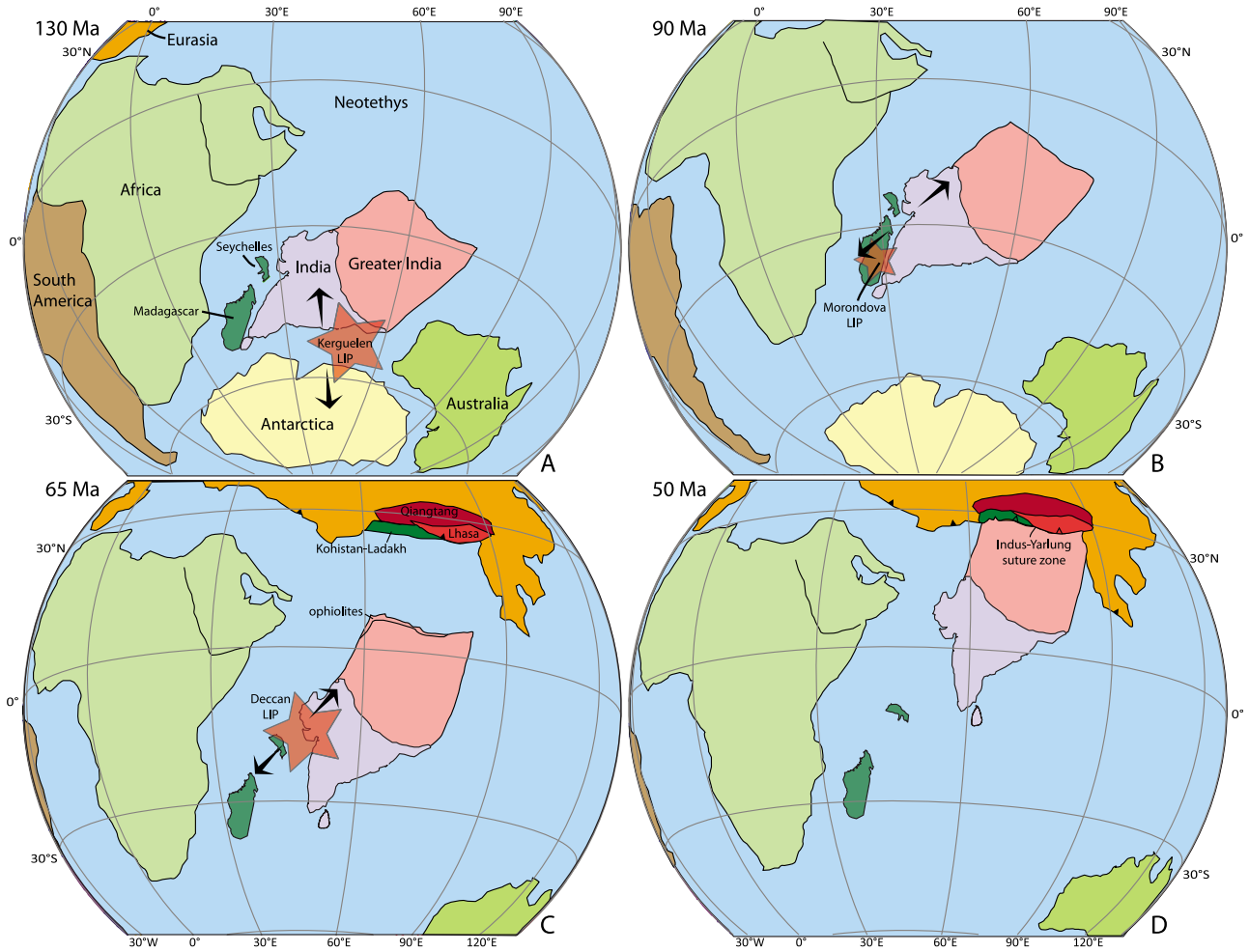

Figure 1. Plate reconstructions showing the configurations of India at (a) 130 Ma, at the initiation of the India-Antarctica/Australia separation and the onset of the Kerguelen LIP; (b) 90 Ma, at the initiation of Madagascar-India separation and the onset of the Morondova LIP; (c) 65 Ma, at the initiation of India-Seychelles separation and the onset of the Deccan LIP; and (d) 50 Ma, during the early stages of India-Asia collision. Plate reconstruction from *Torsvik et al.* [2008], in the slab-fitted mantle reference frame of *van der Meer et al.* [2010] with the location of the pre-50 Ma southern margin of Asia, and a size of Greater India defined by assuming a 50 Ma Tethyan Himalaya-Lhasa collision and a total of 650 km of intra-Asian shortening to the east and 1050 km to the west of the Karakoram Fault-Kashgar-Yecheng transfer system (see text for further explanation).

ation of seafloor spreading between India and Antarctica-Australia [*Gaina et al.*, 2003, 2007]. This was followed by further separation between India and Madagascar (~90 Ma) and India and the Seychelles (~65 Ma) mentioned above (Figure 1). In our analysis of the effects of mantle plumes on relative convergence rates we therefore limit ourselves to the last 130 Ma, when we can speak of an Indian plate.

[14] Since the collision between India and Asia, ongoing convergence led to shortening of the overriding Asian plate, and subduction (and upper crustal accretion) of the Indian plate. The area of Asian plate that was consumed by shortening since collision is commonly referred to as "Greater Asia," and the area of subducted Indian Plate since collision as "Greater India." The northernmost continental sediments that were derived from Greater India are found today in the Tethyan Himalayas.

[15] Since 130 Ma, subduction zones existed to the north of the Indian continent, accommodating India-Eurasia convergence. A long-lasting subduction zone consuming Neotethyan oceanic crust between India and Asia, occurred since ~130 Ma below the southernmost continental terrane of Tibet – the Lhasa terrane. The Lhasa terrane collided around ~140–130 Ma ago with the Qiangtang terrane to its north, which had been part of Asia since the earliest Jurassic [*Dewey et al.*, 1988; *Hsü et al.*, 1995; *Kapp et al.*, 2000, 2007a; *Yin and Harrison*, 2000]. A geological record of the Cretaceous subduction history below Asia is provided by a long-lived Cretaceous-Eocene volcanic arc on the Lhasa terrane: the Gangdese arc [e.g., *Ji et al.*, 2009].

[16] The suture zone between India and Asia contains obducted ophiolites, which were emplaced onto the Tethyan Himalayan crust at the Greater Indian continental margin [e.g., *Gnos et al.*, 1997; *Corfield et al.*, 2001; *Ding et al.*,

2005; *Guilmette et al.*, 2009; *Searle and Treloar*, 2010]. This indicates that intraoceanic subduction occurred, followed by obduction of the overriding oceanic crust onto Tethyan Himalayan crust when Greater India arrived in that subduction zone, prior to the continent-continent collision between Tethyan Himalayan lithosphere and the Lhasa terrane.

[17] For our analysis, it is critical to assess when continental lithosphere of the Indian plate entered a subduction zone. We stress, that a deceleration of the India-Asia collision may result from continental subduction, regardless whether the overriding plate is oceanic or continental. Therefore, we provide a short review on the current ideas on the timing of Indian plate subduction events since 130 Ma, and outline existing controversies.

[18] In the NW Himalaya, intraoceanic subduction appears to have commenced ~100–90 Ma below the Spontang ophiolite, overlying the northwest Himalayas, as well as below ophiolites in Pakistan (e.g., the Dras ophiolite) [*Corfield et al.*, 2001; *Searle and Treloar*, 2010]. Emplacement of these ophiolites and overlying arcs onto Greater India is not beyond controversy, but was postulated to occur between 75 and 65 Ma, in one or more phases [*Gnos et al.*, 1997; *Corfield et al.*, 2001; *Searle and Treloar*, 2010]. A similar, ~95 Ma age for onset of intraoceanic subduction was reported from the Andaman ophiolites to the west of Indochina [*Pedersen et al.*, 2010]. Because of the similarity between these ages for onset of intraoceanic subduction below ophiolites in the India-Asia collision zone and ages from a belt of ophiolites stretching from Turkey and Cyprus, through Syria and Iran to Oman, e.g., *Pedersen et al.* [2010] argued for the existence of a continuous, Tethys-wide Cretaceous intraoceanic subduction zone, in which Arabia and Greater India arrived approximately 75–65 Ma ago with consequent ophiolite obduction and slab break off. This suggestion is in line with seismic tomographic images of the sub-Indian mantle that lend support for several, perhaps simultaneously active subduction zones in the Neotethyan ocean between India and Asia since 130 Ma [*Hafkenscheid et al.*, 2006; *van der Meer et al.*, 2010].

[19] Metamorphic rocks below the Xigaze ophiolites in the Indus-Yarlung suture southwest of the city of Lhasa, have been interpreted to reflect metamorphic soles, and have yielded ~130–120 Ma $^{40}Ar/^{39}Ar$ ages [*Guilmette et al.*, 2009], an age close to the onset of subduction below the Lhasa terrane and activity of the Gangdese arc. These metamorphic soles probably reflect the onset of subduction of Neotethyan oceanic crust below oceanic crust that is represented by these ophiolites. The difference of these ages with the ~100–90 Ma onset ages reviewed above may indicate an origin in a different subduction zone, and consequently a different age of obduction. There is a general agreement that around 55–50 Ma, continental lithosphere of Greater India, carrying the sedimentary rocks now found in the Tethyan Himalayas, arrived in a subduction zone. Supporting evidence for entrance of Greater India in a subduction zone around 55–50 Ma comes especially from the age of the oldest (U)HP metamorphic terrigeneous clastic metasediments of the Indian plate below the Indus-Yarlung suture zone of 54–50 Ma [*Leech et al.*, 2005; *Guillot et al.*, 2008]. In addition, several authors argue for a cessation of continuous open marine sedimentation in the northwestern Tethyan Himalayas below the Indus-Yarlung ophiolites around 52–50 Ma [*Rowley*, 1996; *Najman and Garzanti*, 2000; *Najman et al.*, 2005, 2010; *Green et al.*, 2008].

[20] This age, however, is not beyond controversy. *Wang et al.* [2002] assigned a 34 Ma age for the top of the key Qumiba section in the Tethyan Himalayas, as opposed to the ~52–50 Ma age assigned to the same section by *Zhu et al.* [2005] and *Najman et al.* [2010], but even if younger marine sediments are found south of the Indus-Yarlung suture zone, that does not exclude collision (compare, e.g., the Persian Gulf on continental Arabia, which is still marine despite Arabia-Eurasia continent-continent collision since at least the early Miocene [e.g., *Agard et al.*, 2005].

[21] Furthermore, the age of the UHP metamorphism indicates an onset of continental Indian plate subduction, but does not define the nature of the overriding plate. Therefore, the controversy on the age extends to whether this continental subduction occurred below oceanic crust represented by the Xigaze ophiolites, or whether this represents the Tethyan Himalaya-Lhasa collision. *Ali and Aitchison* [2006] and *Aitchison et al.* [2007] argued that Tethyan Himalaya-Lhasa continent-continent collision occurred much later, around 34 Ma, and these authors suggested that a wide oceanic domain remained between the Tethyan Himalayas and the Lhasa terrane after a ~55–50 Ma collision between an intraoceanic arc and the Tethyan Himalayas. They argued that Tethyan Himalaya-Lhasa continent-continent collision occurred much later, around 34 Ma, referring to the youngest marine sediments from the Qumiba section as dated by *Wang et al.* [2002] (but see the controversy outlined above), and by suggesting that the global synthetic Apparent Polar Wander Paths (APWPs) of *Torsvik et al.* [2001], *Besse and Courtillot* [2002], and *Schettino and Scotese* [2005] are incorrect for Eurasia. Instead, they chose alternative paleomagnetic poles, placing Eurasia >1000 km further north. However, as pointed out by *Dupont-Nivet et al.* [2010b], they considered the same global synthetic APWP as essentially correct for India, thereby suggesting that Eurasia was decoupled from the plate circuit in the early Cenozoic. Their preferred poles would create a large overlap between Eurasia and North America, which is not in line with geological evidence.

[22] According to *Ding et al.* [2005], the overriding oceanic plate from which the Xigaze ophiolites were derived was only very narrow, and they suggested a direct relationship between the Neotethyan subduction zone below the Indus-Yarlung ophiolites, and the Cretaceous Gangdese volcanic arc. In that scenario, the collision between the Tethyan Himalayas and the ophiolites is directly followed by continent-continent collision. This interpretation seems to be supported by the recognition of detrital zircons with Cretaceous to earliest Eocene ages interpreted to come from the Gangdese arc in 52–50 Ma clastic marine detritus in the Tethyan Himalayas [*Najman*, 2006; *Najman et al.*, 2010].

[23] To test these scenarios, five paleomagnetic studies were recently published [*Chen et al.*, 2010; *Dupont-Nivet et al.*, 2010a; *Liebke et al.*, 2010; *Sun et al.*, 2010; *Tan et al.*, 2010] in addition to an earlier study of *Achache et al.* [1984], which aimed to constrain the collision age by comparing paleolatitudes from the Tethyan Himalayas published by *Patzelt et al.* [1996] (corrected for compaction-induced inclination shallowing by *Dupont-Nivet et al.* [2010b]) with

newly obtained data from the ~50 Ma old Linzizong volcanics that cover large parts of the Lhasa terrane. Surprisingly, these studies provided a wide range of collision ages from ~60 to ~40 Ma, mainly owing to low numbers of data points and consequently underrepresentation of paleosecular variation. *Lippert et al.* [2010] averaged all these paleomagnetic data from the Linzizong volcanics, showed a positive fold test, a positive reversal test and a data dispersion consistent with paleosecular variation. They concluded a 48 ± 8 Ma collision age, noting that this should be regarded as a minimum age, because shortening in the Xigaze forearc, subduction of the northern passive margin of the Tethyan Himalayas and shortening of the Tethyan Himalayas north of the sites of *Patzelt et al.* [1996] is unaccounted for in this analysis. These data seem to suggest that the continental subduction episode starting around 55–50 Ma below the Xigaze oceanic crust first emplacing ophiolites, very soon followed by continent-continent collision.

[24] Figure 1 shows time slices of the India-Asia plate configuration since 130 Ma. The size of Greater India in these reconstructions is much larger than previously argued for [e.g., *Lee and Lawver*, 1995; *Ali and Aitchison*, 2005]. As defined above, Greater India is the amount of Indian Plate lithosphere that subducted (with or without accretion) since the collision between the Tethyan Himalayas and the Lhasa terrane. Its size is hence defined by the age of collision, and the amount of intra-Asian shortening since that time. Our size of Greater India is based on the assumption of a 50 Ma collision age, with reference to the arguments listed above. The amount of intra-Asian shortening based on structural geological criteria from Tibet, the Tien Shan and Mongolia has consistently been estimated at some 600 km [*Dewey et al.*, 1988; *Yin and Harrison*, 2000; *Johnson*, 2002; *Guillot et al.*, 2003]. More recent estimates for post-50 Ma shortening within Asia indicate (1) a total amount of ~400 km of shortening within Tibet, with 15% shortening for the Lhasa terrane, 25% for the Qiangtang terrane and 50% for the Songpan Garzi terrane [*Spurlin et al.*, 2005; *Kapp et al.*, 2005, 2007a, 2007b]; (2) a ~150 km N-S shortening component associated with 400–500 km of left-lateral motion along the 070°E striking Altyn Tagh fault, partitioned into transpression along its northeastern and southwestern terminations [*Cowgill et al.*, 2003; *Yue et al.*, 2005], and (3) up to 200 km of shortening in the western Tien Shan, decreasing to only some tens of kilometers in the east, distributed across Mongolia [*Avouac et al.*, 1993; *Yin et al.*, 1998; *Cunningham*, 2005]. These estimates yield a similar total amount of shortening of ~650 +/− 100 km since 50 Ma. In the Pamir-Hindu Kush region, which is separated from Tibet along the right-lateral Karakoram Fault and Kashgar-Yecheng transfer fault systems, shortening must have been at least ~400 km more, as suggested by a ~110–150 km displacement along the Karakoram Fault [*Schwab et al.*, 2004; *Searle and Phillips*, 2007; *Robinson*, 2009] and a ~270 km displacement along the Kashgar-Yecheng transfer system [*Cowgill*, 2010]. In our reconstruction we hence apply a Greater Asia of ~650 km east of the Karakoram Fault and ~1050 km to its west.

[25] We note that an alternative view on intra-Asian shortening exists, which predicts large-scale extrusion of the Indochina block along the Aliao Shan–Red River Fault (ASRRF) over a distance of 700 ± 200 km from between the Qiangtang and Lhasa terranes [e.g., *Peltzer and Tapponnier*, 1988; *Leloup et al.*, 1995; *Royden et al.*, 2008], which also involves much larger displacements along the Karakoram Fault of up to 500 km [e.g., *Lacassin et al.*, 2004; *Valli et al.*, 2007]. The regional geometrical consequences of this scenario was modeled by *Replumaz and Tapponnier* [2003], who demonstrated that such large-scale extrusion requires ~500 km E-W extension in Tibet between ~30 and 15 Ma, and ~500 km of contemporaneous N-S shortening of the Lhasa terrane, and ~500 km of left-lateral strike slip between the Lhasa and Qiangtang terranes. This contradicts with the very minor shortening recorded in the regionally flat-lying Linzizong volcanics that cover large parts of the Lhasa terrane [*Kapp et al.*, 2007b], and the much younger onset, and much smaller amounts of E-W extension in Tibet [e.g., *Kapp and Guynn*, 2004]. The Cretaceous to Paleogene fold-thrust belt that straddles the suture between the Qiangtang and Lhasa terranes is not affected by strike-slip faults with displacements of more than several kilometers [*Taylor et al.*, 2003; *Kapp et al.*, 2005]. In addition, *Searle* [2006] challenged the interpretation of such major displacements along the ASRRF and *Hall et al.* [2008] showed that only ~265 km of extrusion can be reconciled with the geology of Indonesia. Moreover, they demonstrated that the extrusion modeled by *Replumaz and Tapponnier* [2003] leads to an almost complete overlap between the west Burma block and Indochina. Finally, the full extrusion scenario requires a palinspastic position of Indochina south of Qiangtang and thus widely contradicts the early Jurassic age of the Qiangtang collision with Asia and the late Triassic age of the Indochina-South China suture [*Yin and Harrison*, 2000; *Cai and Zhang*, 2009]. Therefore, we do not follow the extrusion scenario as a viable alternative for accommodating significant amounts of the Indo-Asia convergence.

[26] The consequent size of Greater India in the reconstruction of Figure 1 is much larger than the amount of shortening of ~600–900 km recorded in the Himalayas [*DeCelles et al.*, 2002; *Long et al.*, 2011, and references therein]. A discussion of this long-standing controversy is beyond the scope of this paper, but in general two end-member scenarios exist: either collision was much younger [*Aitchison et al.*, 2007], or a large part of Greater India subducted without leaving a geological record at the surface, either by duplexing below the Tibetan plateau, or by wholesale subduction. The latter option would suggest that the Greater India may not have been entirely continental [*Hsü et al.*, 1995; *Dupont-Nivet et al.*, 2010a].

[27] In summary, since 130 Ma, the Indian plate was surrounded by oceanic spreading centers in the south, and subduction zones in the north. An ocean basin formed between India and Madagascar starting around ~90 Ma, associated with emplacement of the Morondova LIP, and the Indian plate fragmented due to separation of India from the Seychelles around ~65 Ma, in space and time related with emplacement of the Deccan LIP. Perhaps following a late Cretaceous phase of arc-continent collision and associated ophiolite emplacement, an important continental subduction episode started around 55–50 Ma, first emplacing ophiolites, (soon) followed by continent-continent collision. It is these two episodes, the postulated late Cretaceous, and particularly the better constrained Eocene Indian plate

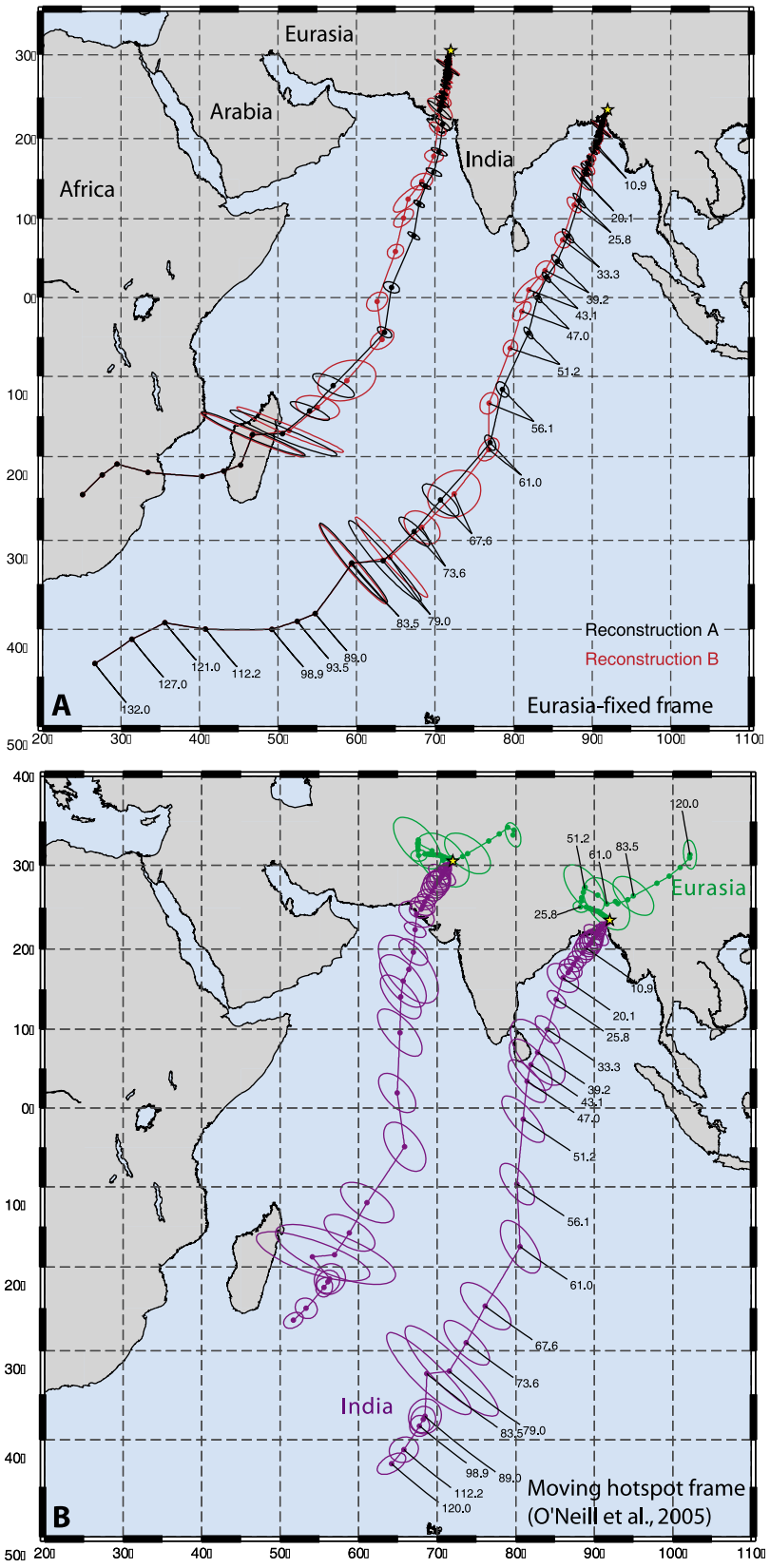
Eurasia
Arabia
India
Africa
10.9
20.1
25.8
33.3
39.2
43.1
47.0
51.2
56.1
61.0
67.6
73.6
79.0
83.5
89.0
93.5
98.9
112.2
121.0
127.0
132.0
Reconstruction A
Reconstruction B
A
Eurasia-fixed frame
120.0
51.2
61.0
83.5
Eurasia
25.8
10.9
20.1
25.8
33.3
39.2
43.1
47.0
51.2
56.1
61.0
67.6
73.6
India
79.0
83.5
89.0
98.9
112.2
120.0
B
Moving hotspot frame
(O'Neill et al., 2005)

Figure 2

continental subduction events that we will focus on in our further analysis.

3. Kinematics of India-Asia Relative Motion and Absolute Indian Motion

[28] Relative motions between India and Eurasia since late Cretaceous time were calculated using a chain of relative motion (plate circuit) that combines reconstructions of India relative to Africa (Somalia), Africa to North America, and North America to Eurasia, including estimates of deformation within the African composite plate (i.e., Somalia-Nubia motion along the East African Rift during Neogene time and Cretaceous motion between northwest Africa and the South African craton).

[29] When reconstructing plate motions through a plate circuit, it is always desirable to put uncertainty bounds on the amount of calculated displacement. Hence, in our selection of rotation parameters for individual reconstructions involved in the India-Eurasia circuit, we naturally gave preference to those studies that estimated reconstruction uncertainties through a formal statistical analysis [e.g., *Stock and Molnar*, 1983; *Stock et al.*, 1990]. The geomagnetic polarity timescale calibrations of *Gradstein et al.* [1994] and *Cande and Kent* [1995] were used to assign absolute ages in all individual reconstructions, with a switch point from the Late Cretaceous-Cenozoic timescale [*Cande and Kent*, 1995] to the Mesozoic timescale [*Gradstein et al.*, 1994] set to the younger edge of the Cretaceous Normal Superchron, at 83.5 Ma, following *Torsvik et al.* [2008]. In the following discussion of sources for individual reconstructions, we will use the polarity chron notation of *Cande and Kent* [1995], the "y" and "o" following the chron identifier denoting the young and old edges of the chron, respectively.

[30] The Euler rotation parameters and their uncertainties for the reconstructions included in our plate circuit models are presented in Table S1 of the auxiliary material.[1] To reconstruct the Cenozoic motion of India relative to the Somalian plate, we have used most recent kinematic models of the Indian Ocean closure. These include (1) detailed India-Somalia reconstructions of *Merkouriev and DeMets* [2008] for the last 20 Ma (chron C6no time to the recent), (2) the estimates of Neogene deformation within the Central Indian Basin of *DeMets et al.* [2005] (India-Capricorn motion), and (3) the updated kinematics of Capricorn-Somalia motion recently published by *Cande et al.* [2010] for the time interval between chrons C13o and C29o (33.5–64.7 Ma). For the Late Cretaceous India-Somalia reconstructions (chron C30r-C34y time, 67.7–83.5 Ma), we have adopted the rotation parameters of *Molnar et al.* [1988]. The opening of East African Rift (Somalia-Nubia motion) was reconstructed using the rotation parameters of *Horner-Johnson et al.* [2007] and *Lemaux et al.* [2002]. Similar to a recent study of India-Asia convergence by *Molnar and Stock* [2009], we assumed that active East African rifting began approximately 11 million years ago (chron C5no), and no motion between Somalia and Nubia had occurred prior to that time.

[31] For the closure of the Atlantic Ocean, we considered two alternative models involving different fits between Africa, North America and Eurasia. In the first model (model A), we used the Africa-North America rotations of *Müller et al.* [1999] back to chron C34ny time (83.5 Ma), North America-Eurasia reconstructions of *Gaina et al.* [2002] back to chron C33no time (79.1 Ma), and the North America–Eurasia rotation of *Srivastava and Roest* [1989] for chron C34ny. Model B is essentially the reconstruction choice of *Molnar and Stock* [2009], and uses rotations of *McQuarrie et al.* [2003] to define relative displacements between Africa, North America and Eurasia since chron C30r (67.7 Ma). For earlier time (up to 83.5 Ma), rotations of *Klitgord and Schouten* [1986] were used for the Africa–North America motion and those of *Srivastava and Roest* [1989] for the North America–Eurasia fit.

[32] Extending the reconstruction further back in time, we switched to the India-Madagascar-South Africa-Northwest Africa-North America-Eurasia plate circuit of *Torsvik et al.* [2008] prior to 83.5 Ma [see *Torsvik et al.*, 2008, and references therein for details]. No uncertainties are available for these rotations and no attempt was made to estimate them. However, it is probable that the spatial misfits allowable for these reconstructions have the same order or magnitude as those in the oldest reconstructions (e.g., 83.5 Ma rotations) for the two India-Eurasia motion models discussed above; hence, a cumulative reconstruction error of several hundred kilometers is quite conceivable.

[33] Estimating absolute motions of India and Eurasia relative to the Earth's mantle (Figures 2b, 3e, and 3f), we used our relative plate circuit models to reconstruct India and Eurasia relative to Africa and then added absolute rotations of Africa in the moving Indo-Atlantic hot spot reference frame of *O'Neill et al.* [2005].

[34] Finite rotations were combined and their uncertainties were estimates following the procedure of *Doubrovine and Tarduno* [2008]. The rotation uncertainties parameterized as "partial uncertainty rotations" [*Stock and Molnar*, 1983; *Molnar and Stock*, 1985] in some reconstructions [*Molnar*

[1] Auxiliary materials are available in the HTML. doi:10.1029/2010JB008051.

Figure 2. (a) Flow lines for two points moving with the Indian plate relative to the fixed Eurasia. The present coordinates are 30.5°N, 72°E (western point) and 23.5°N, 92°E (eastern point). Black flow line is calculated using model A reconstruction for the Atlantic Ocean, red line is according to model B, segments corresponding to ages older than 83.5 Ma are identical in both models (see text). Reconstructed positions are shown at select ages; ellipses represent 95% reconstruction uncertainty. Note that reconstruction uncertainties are slightly underestimated for ages older than 79 Ma in model A and 67 Ma in model B because the uncertainties are not available for the rotations of *Srivastava and Roest* [1989] and *Klitgord and Schouten* [1986]. (b) India-Asia convergence flow lines in the moving Indo-Atlantic hot spot reference frame of *O'Neill et al.* [2005] for our preferred reconstruction A. Error bars include the errors of the relative plate reconstruction (unavailable for the reconstruction ages older than 83.5 Ma) and errors associated with the moving hot spot frame of *O'Neill et al.* [2005].

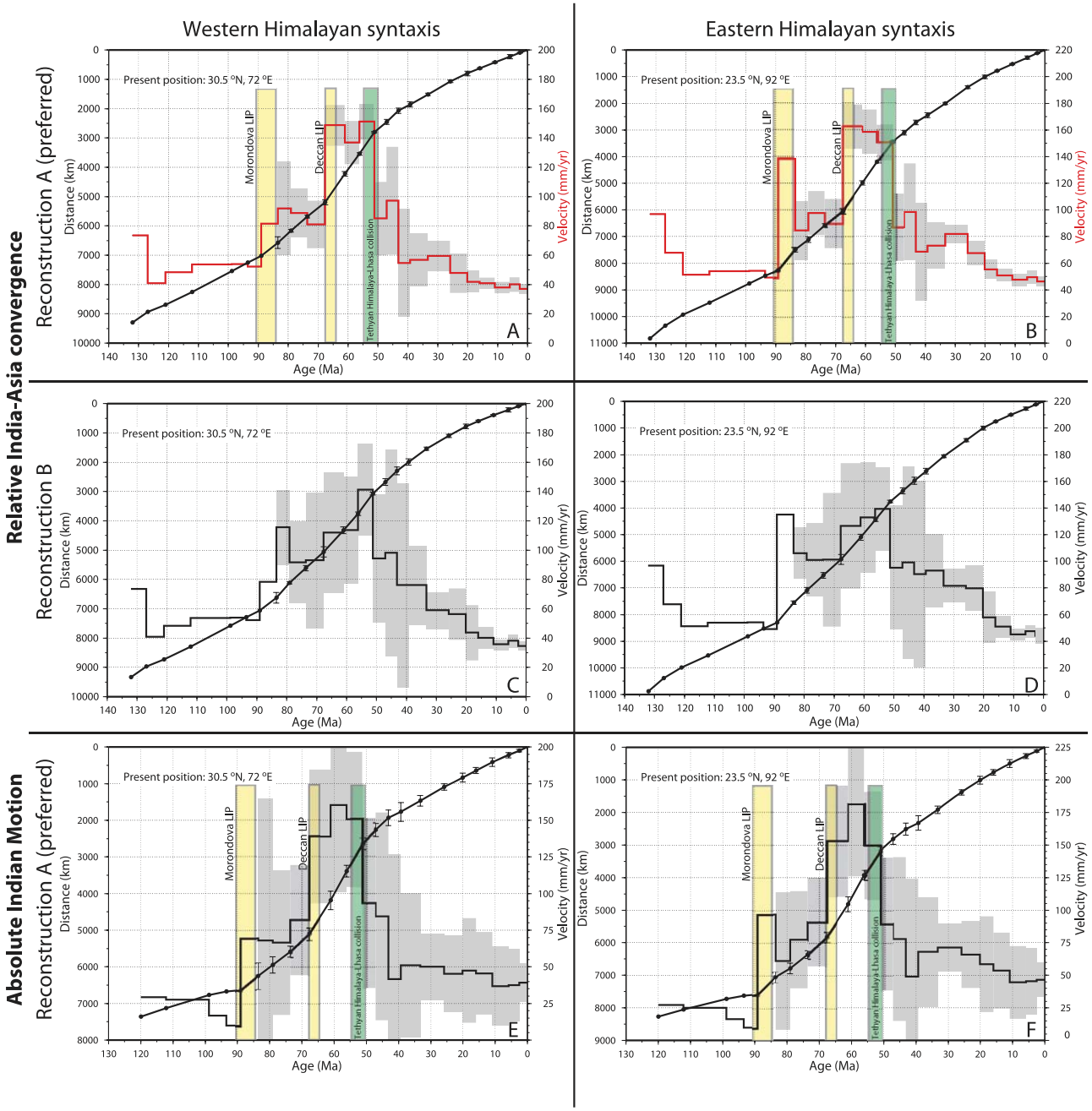

Figure 3. Distances traveled by the Indian plate relative to Eurasia along the two flow lines shown in Figure 2 for (a and b) our preferred model A, western and eastern Himalayan syntaxis, respectively, and (c and d) model B, western and eastern syntaxis, respectively. (e and f) Absolute motion of India with respect to the mantle, using the moving Indo-Atlantic hot spot frame of *O'Neill et al.* [2005], for the preferred reconstruction A. Error bars in Figures 3e and 3f combine the errors of the relative plate reconstruction with the errors of the moving hot spot reference frame of *O'Neill et al.* [2005]. Solid points correspond to the reconstructed positions in Figure 2; error bars are 95% uncertainties. Stepwise line is the velocity of relative motion (first derivative of the distance versus age curve); gray shading shows the 95% uncertainties of velocity estimates. See text for further explanation on models A and B.

et al., 1988; *McQuarrie et al.*, 2003] were recalculated into covariance matrices defined using the moving exponential parameterization of *Chang* [1988]. A common set of ages was compiled, comprising all reconstruction ages from all individual reconstructions included into the plate circuit. If a particular age from this set was not one of the original reconstruction ages for an individual plate pair or plate hot spots reconstruction, the finite rotation corresponding to this age and its uncertainty were estimated by interpolation between the two closest original rotations using the equa-

tions presented by *Doubrovine and Tarduno* [2008]. The interpolation procedure assumes steady plate motion during the time interval between the bracketing ages. Coeval rotations (original or interpolated) were then combined and uncertainty of each combined rotation was estimated using established formulations [e.g., *Stock et al.*, 1990].

[35] The resulting models of India-Eurasia relative motion (Table S1) are illustrated by plotting reconstructed positions of two points moving with the Indian plate, which roughly correspond to the longitudes of the western and eastern Himalayan syntaxes, relative to the arbitrarily fixed Eurasia (Figures 2a and 3a–3d). Absolute motions of the Indian and Eurasian plates in the moving Indo-Atlantic hot spot frame of *O'Neill et al.* [2005] are shown in Figures 2b, 3e, and 3f.

[36] The two alternative models of the Atlantic Ocean closure produce small, but sizable differences in the calculated flow lines of Indian plate motion in the reference frame fixed to Eurasia (Figure 2a). For 83.5 Ma, both models result in virtually identical India-Eurasia rotations. The 79 to 61 Ma reconstructions show larger differences between the two models; these however are not statistically significant at a 95% confidence level. The most notable discrepancies, significantly above the level of reconstruction error, are observed for the 56 to 20 Ma interval. After 20 Ma, the differences between the two models are very small and are not statistically significant.

[37] The main reason for the discrepancies between the two India-Eurasia models is the choice of rotations for the northern Atlantic (the North America–Eurasia reconstructions of *Gaina et al.* [2002], in model A versus rotations of *McQuarrie et al.* [2003], in model B). The two reconstructions of Africa–North America motion [*Müller et al.*, 1999; *McQuarrie et al.*, 2003] are virtually identical, so that using one or the other in any of our models does not alter results significantly. In the following discussion of the India-Eurasia convergence history we will rely on the results from model A. We prefer this model because reconstructions of *McQuarrie et al.* [2003] are based on early compilations of marine geophysical data [*Klitgord and Schouten*, 1986; *Srivastava and Tapscott*, 1986; *Srivastava et al.*, 1990], whereas newer and more comprehensive data sets were used by *Gaina et al.* [2002] and *Müller et al.* [1999], including updated magnetic anomaly databases and satellite-derived gravity data for detailed mapping of fracture zones in the central and northern Atlantic Ocean. Model B nevertheless provides a good illustration on sensitivity of the estimated India-Eurasia motion to the choice of reconstructions in the Atlantic Ocean.

[38] The reconstructed motion displays several important changes in the direction and velocity since Cretaceous time (Figures 2 and 3). During much of the Cretaceous, the motion of India relative to the fixed Eurasia was dominantly eastward and relatively slow, averaging to ~50 mm/yr during the 120–90 Ma interval. At about 90 Ma, the direction of motion changed to northeastward, associated with a counterclockwise rotation of India, illustrated by a temporary increase in velocity ranging from ~80 mm/yr for the western flow line to ~140 mm/yr for the eastern line (Figure 3). A large difference in velocity increase originates from the fact that western India was closer to the stage rotation pole during the 90–84 Ma period. From 83.5 to 79 Ma, the direction returns back to more eastward orientation and velocity for the eastern flow line falls to ~85 mm/yr. The counterclockwise rotation of India at around 90 Ma most likely resulted from the initial opening of the eastern Indian Ocean, with a new spreading ridge propagating northward between India and Madagascar [e.g., *Gaina et al.*, 2003, 2007]. The reason for the following clockwise rotation at 83.5 Ma is not clear. We note, however, that the reconstruction uncertainties for the 83.5 Ma and 79 Ma rotations are large (Figure 2), and it is possible that the 83.5 Ma kink in the calculated flow lines is an artifact of reconstruction error rather than true variation in the direction of motion.

[39] From 79 to 67 Ma, India moved steadily northeast relative to fixed Eurasia with the velocity at an 80–90 mm/yr level. After 67 Ma, the convergence velocity increased dramatically to 150–160 mm/yr but the direction of relative India-Eurasia motion did not change noticeably. This time corresponds to the arrival of the Deccan plume (65.5 Ma) followed by an eastward jump of the spreading ridge that transferred the Seychelles microcontinent from India to the African plate at about 61 Ma [e.g., *Gaina et al.*, 2003; *Ganerød et al.*, 2011]. Coincidentally, at 61 Ma, the direction of motion changed to a NNE orientation, but the velocity remained at similarly high levels (130–180 mm/yr) up until 51 Ma, after which it dropped rapidly to ~60–70 mm/yr around 40 Ma. Interestingly, the 50 Ma slowdown of the India-Eurasia convergence, traditionally interpreted as the onset of the India-Asia continent-continent collision [e.g., *Patriat and Achache*, 1984], did not have any appreciable effect on the direction of relative motion, which continued steadily in the NNE direction up to Recent. After 40 Ma, the India-Eurasian convergence was gradually slowing down (Figure 3), reaching 40–50 mm/yr at about 20 Ma, and remaining on this level since that time.

[40] The description of convergence history above is according to model A, which we favor. Model B suggests a somewhat different picture (Figure 3). The main difference is that the 67–51 Ma velocity spike is less pronounced overall, and the velocity increases rather gradually after 67 Ma to reach the maximum during 56–51 Ma interval. The latter contrasts with the sudden velocity increase at 67 Ma followed by a plateau up until 51 Ma. Additionally, model B produces a small but noticeable drop in velocity at 20 Ma, consistent with *Molnar and Stock* [2009], whereas model A suggests a smoother decrease in the convergence velocity over the last 40 Ma. We also note that using the *Gradstein et al.* [2004] timescale instead of *Cande and Kent* [1995] does not significantly change the estimated values, and the description given above is valid regardless of the timescale choice.

[41] The motion of India in the Indo-Atlantic hot spot reference frame (Figure 2b) exhibits changes in absolute velocity similar to those observed in the relative India-Eurasia reconstructions, with two episodes of acceleration around 90 and 67 Ma followed by a sharp slowdown between ~50 and 40 Ma (Figure 3). The absolute India motion was dominantly to the NNE during the Cretaceous and the earliest Paleogene (120–61 Ma), changed to a nearly northward direction between 61 Ma and 40 Ma, and then gradually returned to the NNE direction. The main difference with the motion of India relative to Eurasia is a smaller eastward component of absolute motion for the 120–51 Ma interval, especially its earlier 30 million years (~120–90 Ma),

Table 1. Model Parameters for Code 1 and CitcomS

Model Parameter	Code 1	CitcomS
Earth radius, r_E	6371 km	6371 km
Mantle thickness	2900 km	2900 km
Surface density anomaly	+1%	0%
CMB density anomaly	−0.7%	−1.5%
Gravity, g	10 m/s	10 m/s
Thermal expansivity,[a] α	2×10^{-5}/K	3×10^{-5}/K
Heat capacity,[a] c_P	1250 J/kg/K	1200 J/kg/K
Thermal diffusivity, κ	30 km^2/Myr	31.5 km^2/Myr
Internal heating term, $\alpha\rho H/c_p$	0	0
Impedance factor, $\tau/A/\omega/r_E$	2.067 MPa/(deg/Myr)	2.775 MPa/(deg/Myr)

[a]In the case of the code 1, values for thermal expansivity and heat capacity only enter the conversion from anomalous mass flux to heat flux in Figure 6 and hence correspond to depth 900 km only.

which is related to dominantly westward absolute motion of the Eurasian plate during this period (Figure 2b). Finally, we observe that the post-50 Ma slowdown of Indian plate motion is even more pronounced in the moving Indo-Atlantic hot spot reference frame, because between ~50 and 25 Ma, Eurasia moved southward with respect to the mantle (Figures 2b, 3e, and 3f).

4. Numerical Modeling of Plume-Plate Interaction

4.1. Method

[42] Plate motions caused by a mantle plume are approximately computed with a two-step approach: In the first step, the plume is numerically modeled and stresses acting at the lithosphere are computed with a fixed upper boundary. These stresses are integrated to torques for given plate geometry. In the second step, the torques are converted to plate angular velocities. This is done in a rather approximate fashion, using a scalar conversion factor or "impedance" described below. A more accurate treatment would require to also consider the interaction between different moving plates [e.g., *Ricard and Vigny*, 1989]. However, these are weaker than the interaction of plates with the underlying mantle, and our approach is sufficient for our purpose, since we are here only interested in an approximate estimate. Our approach essentially considers that torques on plates have to be balanced and determines (in a simplified way, not considering the interaction between plates across boundaries and through the mantle) the plate velocity for which this is the case. We use two different codes (referred to as code 1 and CitcomS) that solve for conservation of mass, momentum and energy with Newtonian viscous rheology for numerical modeling of plumes. Equations for conservation of mass and momentum are

$$(\rho u_i)_{,i} = 0 \tag{1}$$

$$-p_{,i} + \left(\eta\left(u_{i,j} + u_{j,i} - {}^2/_3 u_{k,k}\delta_{ij}\right)\right)_{,i} - \delta\rho g \delta_{ir} = 0 \tag{2}$$

where ρ is (reference) density, u is velocity, p is pressure, η is viscosity, δ_{ij} is the Kroneker delta tensor, $\delta\rho$ is the density anomaly, g is the gravitational acceleration, subscript i symbolizes spatial component i and subscript ,i derivative in direction of i. That means we consider the density anomalies only for the buoyancy force term (last term) in the momentum equation, not in the conservation of mass equation. The momentum equation contains a pressure gradient term, a viscous term and a buoyancy term. The viscous term is for a Newtonian viscous rheology, the buoyancy term for vertical gravity (symbolized by δ_{ir}). Other force terms (including inertial, Coriolis and centrifugal) are not considered.

[43] The conservation of energy equation is

$$T_{,t} + u_i T_{,i} = \kappa T_{,ii} + H/c_p + \alpha g u_r T/c_p + \phi/(\rho c_p) \tag{3a}$$

whereby T is the temperature, κ is thermal diffusivity, c_p is heat capacity, H is the heat production rate, α is thermal expansivity, subscript r symbolizes radial direction, and Φ is viscous dissipation. Model parameters are listed in Table 1.

[44] The left-hand side corresponds to advection, the terms on the right hand side to thermal diffusion, heat production, the difference between adiabatic heating and cooling and viscous dissipation.

[45] The first code (code 1) computes incompressible flow in a spherical shell with a spherical harmonic expansion [*Hager and O'Connell*, 1981] up to degree and order l = 127. A test run with l = 255 yielded only small differences, indicating that l = 127 gives sufficient resolution. The PREM [*Dziewonski and Anderson*, 1981] lower mantle parameters are used for the reference density profile $\rho(r)$. This code only allows for radial viscosity variations, and we use the viscosity structure M2b of *Steinberger and Calderwood* [2006].

[46] For each degree and order, the equations (1) and (2) governing instantaneous flow reduce to a system of ordinary differential equations as a function of radius. Starting from initial values corresponding to the bottom boundary condition, three independent solutions of the homogeneous equation and one solution of the inhomogeneous equation are propagated to the top boundary. The general solution is the sum of the inhomogeneous solution and a linear combination of the homogeneous solutions, and the three free parameters of the general solution are determined by matching the top boundary conditions. The appropriate boundary condition at the core-mantle boundary (CMB) is free slip, but we find that for spherical harmonic degrees higher than about l = 50, solutions grow rapidly with radius to very large values, and the solution matching the top boundary conditions cannot be determined due to numerical roundoff. We circumvene this problem by using a no-slip boundary at depth 50/l × 2900 km for l > 50. In the lowermost mantle, the solution is hence only expanded up until degree 50. Since the modeled plumes are rather thick in the high-viscosity lower mantle (with very little power for degrees l > 50; see Figure 1) this modification affects the solution in only a very minor way.

[47] Solving the equation for the conservation of energy (3a) allows us to compute the evolution of thermal density heterogeneities forward in time. Here we do not explicitly consider temperatures, but instead advect absolute thermal density anomalies $\delta\rho_{th} = T\alpha\rho$; that is, thermal expansivity is implied to vary with radius proportional to $1/\rho(r)$. Also, the terms for viscous dissipation and the difference between

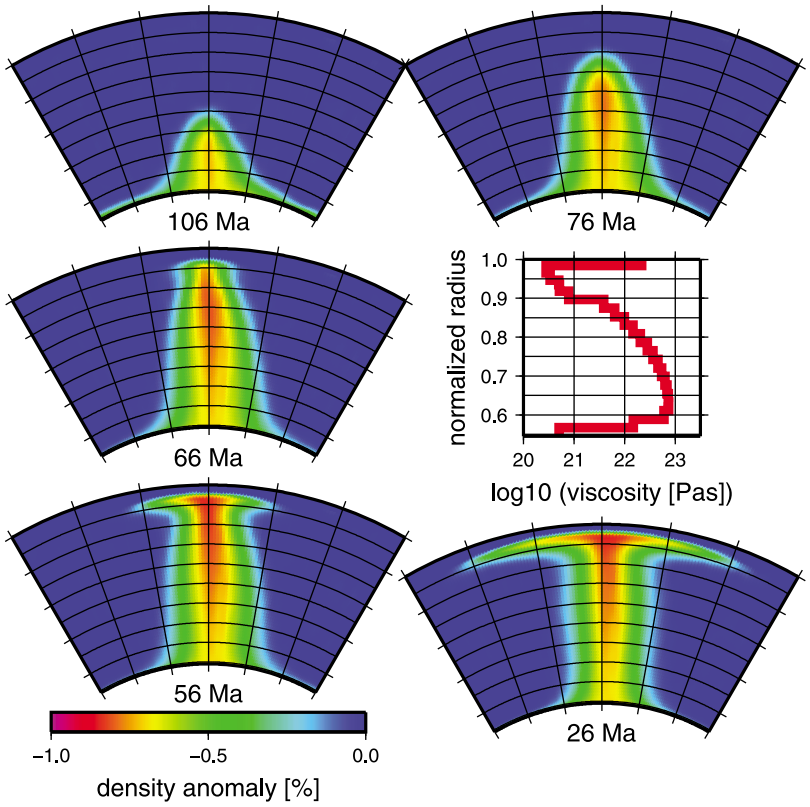

Figure 4. Model cross section through the Deccan plume at different times for code 1 and radial viscosity structure. The cross sections are N-S at 54°E from 54°S to 6°N. They were chosen such that they approximately go through the plume center, but this is not possible at all times and depths, as the plume is not exactly vertical and slightly moves, due to the influence of plumes developing elsewhere in the model, which is global and 3-D. Plumes arrive with an appropriate density anomaly of about −0.9% beneath the lithosphere.

adiabatic heating and cooling are not considered here. Instead of solving equation (3a) we hence solve

$$\delta\rho_{th,t} + u_i\delta\rho_{th,i} = \kappa\delta\rho_{th,ii} + \alpha\rho H/c_p \qquad (3b)$$

The internal heating term $\alpha\rho H/c_p$ is set zero here. This term has only a very minor effect on the plume structure, which we are concerned about in this paper.

[48] For the initial condition, we choose a mantle density model with small random fluctuations on the grid points between −0.1% and 0.1% relative density anomaly. We add a small negative density anomaly in the lowermost mantle around either 23°S, 52°E or 46.9°S, 37.8°E (i.e., below Marion Island following *Torsvik et al.* [1998]), in order to "seed" plumes at locations approximately where the Deccan traps and the Morondava LIP initially erupted. This localized anomaly is chosen to be $-0.35\% \times 0.6^{n-1} \times \exp(-(d/d_0)^2)$, whereby n is the radial layer, d is the distance to the plume location, $d_0 = 6°$. This is sufficiently small such that the size of the plume is not influenced by it, but develops according to its own dynamics. Starting from the initial condition, we forward model the thermal density structure and hence the development and rising of a "mantle plume" due to diffusion of heat into the mantle and subsequent advection. We model the bottom thermal boundary layer by imposing a density anomalies −0.7% in the lowermost layer model at the CMB and +1% in the uppermost layer at the surface. Both advection and diffusion are computed on a grid (59 equally spaced radii from CMB to surface with 50 km distance; 128 Gaussian latitudes; 256 equally spaced longitudes). Hence it is necessary to go back and forth between the space domain and the spherical harmonic domain at each time step. Diffusion is considered only in radial direction with thermal diffusivity 30 km^2/Myr. Advection is computed with an upwind differencing scheme [*Press et al.*, 1986], keeping absolute density anomalies constant during advection: Density $\rho(r)$ increases with depth, hence advecting absolute density anomalies instead of temperatures in the energy equation corresponds to thermal expansivity decreasing with depth $\sim 1/\rho(r)$. On one hand, actual thermal expansivity may decrease even more strongly [e.g., *Schubert et al.*, 2001]. On the other hand, the temperature contrast between plume and surrounding mantle may be higher at larger depth, even in the limit of large plumes when temperature profiles are adiabatic both in the plume and ambient mantle [e.g., *Albers and Christensen*, 1996]. Therefore we regard advecting absolute density anomalies as reasonable approximation. When integrating stresses to compute torques acting on plates, we consider both normal stresses (leading to "downhill forces") and tangential stresses at the base of the lithosphere in 100 km depth, as in the work of *Steinberger et al.* [2001]. Also, in order to remove

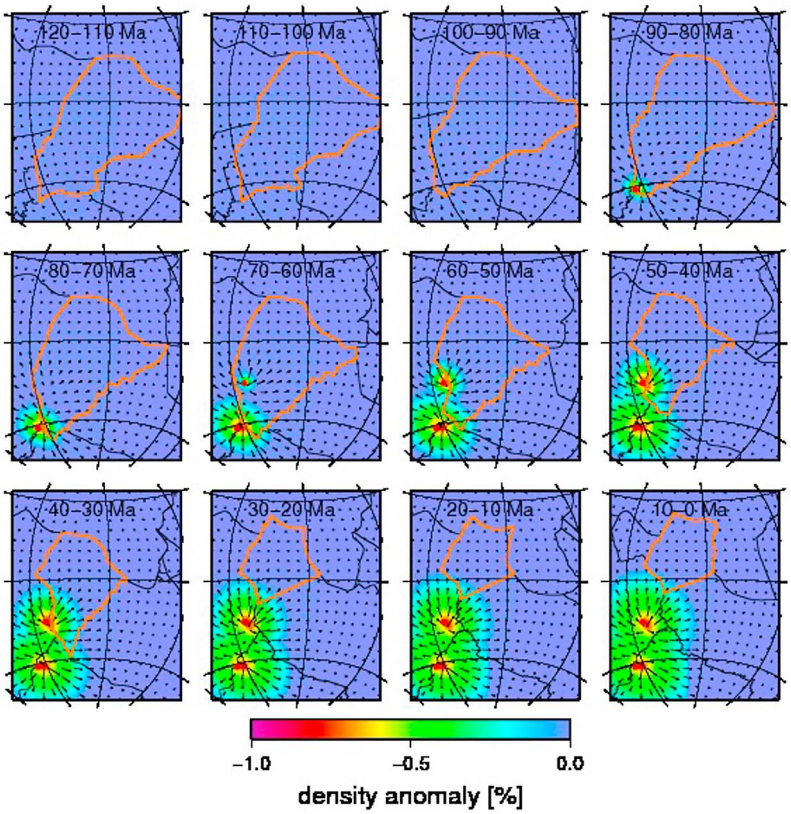

Figure 5. Marion and Reunion plume locations (red dots) relative to the India plate outlined in orange. Colors indicate upper mantle density anomalies (vertically averaged for depths >100 km and <410 km) at times 116 Ma, 106 Ma, etc. Arrows indicate horizontal flow speeds at depth 250 km at the same times, with arrow length corresponding to amount of motion in 10 Myr. Note that the flow computations were done separately for the two plumes. Here we show the linear superposition of the two flow fields and whichever of the two density anomalies is more negative.

the effect of other plumes that develop later at other (random) locations, we compute stresses at each time step only from those density anomalies within a region that contains the "intended" plume and no other plumes (i.e., setting density anomalies outside the region to zero when computing stresses).

[49] For converting resulting torques to plate velocities, we additionally compute the "kinematic" torque τ_{kin} (i.e., without considering any internal density heterogeneities) around the x axis (0°N, 0°E) for the India plate (taken in its 80–90 Ma geometry from *Torsvik et al.* [2010], with area $A_{80–90}$) rotating around the same x axis with 1°/Myr (i.e., moving approximately northward with about 11.1 cm/yr, as it is located around 90°E). Torques τ computed from plumes are hence converted to plate rotations ω (in units of deg/Myr) by dividing through τ_{kin} normalized to plate area:

$$\omega = (\tau/A)/(\tau_{kin}/A_{80-90}) \quad (4)$$

The factor $\tau_{kin}/A_{80–90}$ divided by the Earth radius is determined to 2.067 MPa.

[50] Second, we use the code CitcomS, which is described in detail by *Zhong et al.* [2000] and *Tan et al.* [2006]. The code has been modified in order to allow for the same radial viscosity profile as was used in code 1. Additionally, lateral temperature-dependent viscosity variations are considered as

$$\eta(T) = \eta(z) \times \exp(-14 \times (T - 0.5)) \quad (5)$$

whereby T is dimensionless temperature (varying between 0 and 1; normalizing temperature 1000 K) and which is approximately consistent with the radial viscosity dependence [*Steinberger and Calderwood*, 2006]. Other assumptions are comparable to the first model: The temperature contrast between CMB and mantle is 500 K, which corresponds for the used thermal expansion coefficient of 3×10^{-5}/K to a density contrast of −1.5%. In order to compute the plume heat flux we used a heat capacity of 1200 J/(kg K) and a thermal diffusivity of 31.5 km^2/Myr was used to compute the heat influx at the bottom. However, only tangential stresses are considered here in the computation of the torque. Comparison indicates that both stresses are in a similar direction, with tangential stresses somewhat larger. Hence we expect that including the downhill force in the second model would increase forces and computed plate motions by about 50–100%.

4.2. Results

[51] Results obtained with the spherical harmonic code are given in Figures 4–6, results with CitcomS in Figures 7 and 8.

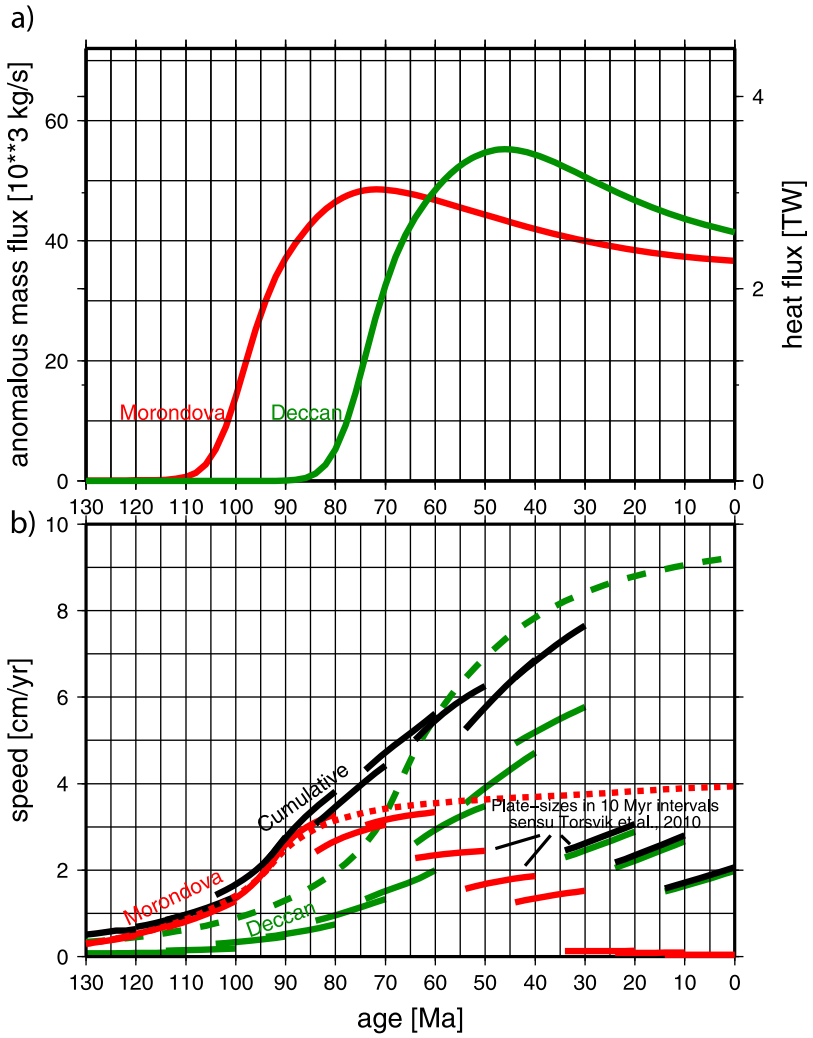

Figure 6. (a) Anomalous mass flux and corresponding heat flux for models of the "Marion" (or Morondava, red) and "Reunion" (or Deccan, green) plume. In this model, the plume head spreads about 1000 km in the 10 Myrs after eruption (average speed 10 cm/yr) and another 1000 km in the following 30 Myrs (average speed 3.3 cm/yr). (b) Computed speed of "free" plate motion caused by the two plumes. Dotted line is speed computed for a plate with the shape of a semicircular "cap," with 47.5 degrees of arc radius (same area as the India plate 80–90 Ma), with the plume impinging at the center of the straight plate boundary, thus transmitting the maximum torque. Dashed line is the same with a smaller cap with 33.7 degrees of arc radius (same area as the India plate 30–40 Ma). Continuous lines show computed with actual plate geometry; velocity component in direction N30E (approximately parallel to transform faults). Red for "Marion," green for "Reunion," and black for the sum of both.

In the first case, ages are assigned such that plumes reach the base of the lithosphere at approximately the right ages when the Deccan and Morondava LIPs erupted (65 and 90 Ma). In the first case, a rather massive plume conduit (typically about 600–700 km diameter at half maximum anomaly) develops, whereas in the second model, where the viscosity inside the conduit is lower, the diameter becomes about 200 km. Anomalous mass flux is computed from density anomalies and velocities in the midmantle (900 km depth in the first model, 725 km in the second model) and converted to heat flux (for the first model, compare the two vertical scales in Figure 6a). The sharp peak in heat flux in the second model can be attributed to the passage of the plume head, whereas in the first model, there is less of a difference between plume head and plume conduit diameter. Maximum heat fluxes computed in both cases are similar around 3–4 TW, in the first case (Figure 6a) they eventually drop to about 2.5 TW, in the second case (Figure 8) to about 0.5 TW. This difference between the two cases can be qualitatively understood as caused by the lower viscosity inside the plume conduit in the second case: Once the plume feeds into the low-viscosity asthenosphere it can "drain" its source region faster and hence its heat flux drops more strongly. We note that heat flux values obtained here are much larger than conventional estimates based on hot spot swells [*Sleep*, 1990; *Davies*, 1988]. But they are more similar to (especially in the second case) recent estimates based on tomography [*Nolet et al.*, 2006]. A lower heat or

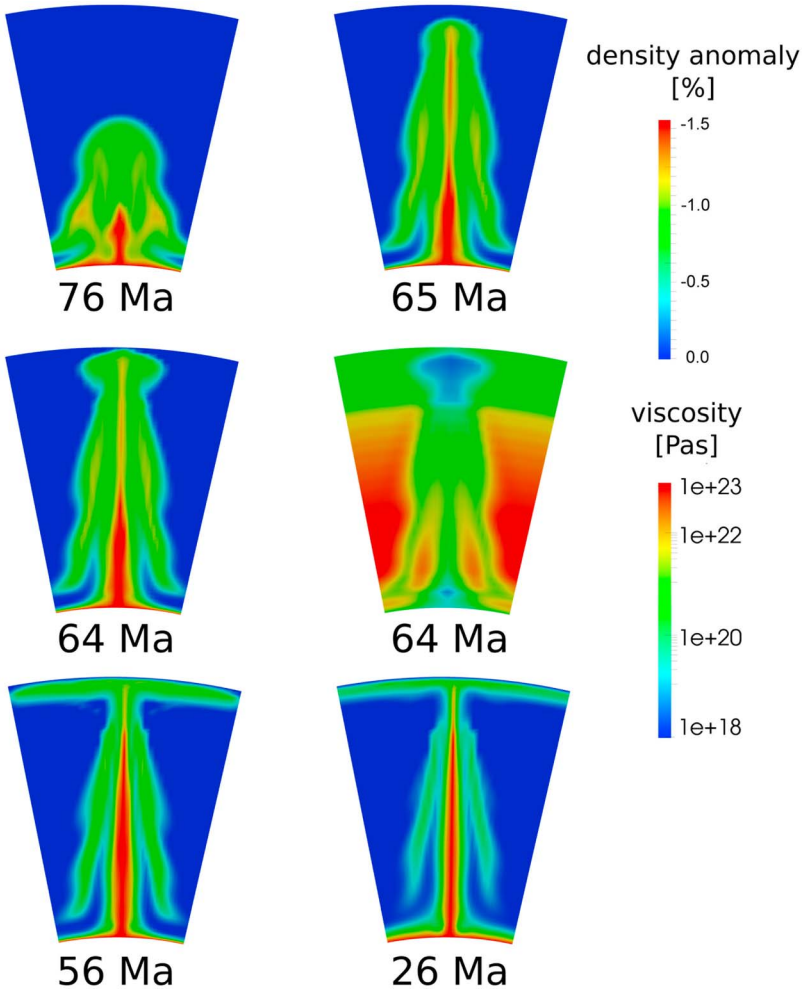

Figure 7. Model cross section through the CitcomS plume model at different times. The right cross section in the middle line shows the temperature-dependent viscosity at the indicated time. Note that the plume decreases viscosity in the asthenosphere significantly (blue section), thus weakening the interaction between lithosphere and asthenosphere. The plume reaches the surface with a density anomaly of slightly more than −1% and a velocity of several tens of centimeters per year, therefore leading to visible movement even in the timescale of a million years.

anomalous mass flux would result with a reduced density and corresponding temperature anomaly assumed as bottom boundary condition: Plumes may start with a lower initial temperature anomaly than the temperature drop across D″, if they rise from the upper part of the edges of chemically distinct piles in the lowermost mantle [e.g., *Torsvik et al.*, 2006]. Estimates of the temperature anomalies of plumes reaching the lithosphere [e.g., *Schubert et al.*, 2001; *Ruedas et al.*, 2004; *Putirka*, 2005] also indicate a lower starting temperature anomaly. The buoyancy flux may also be reduced if plumes entrain chemically heavier material from the lowermost mantle [e.g., *Farnetani and Samuel*, 2005]: an effect that is not modeled here. In any case, what is the appropriate value of plume heat flux is still a matter of debate, but the comparison with other estimates indicates that the following results of resulting plate speeds should probably rather be regarded as an upper limit.

[52] In computing resulting plate speeds we first consider what is approximately the maximum effect. We therefore consider what is the speed that a plume causes if it impinges exactly at the plate edge (dashed and dotted lines in Figure 6b). Results obtained with the spherical harmonic code indicate that plate speed reaches its maximum soon after the plume head has arrived beneath the lithosphere and remains approximately constant after that. Although the anomalous mass flux goes down, the predicted plate speed does not drop, because it is an integrated effect and it continues to remain high as long as the plume head spreads beneath the plate. For a smaller plate size (corresponding to India plate area 30–40 Ma) the maximum speed is about 9 cm/yr, for a larger size (corresponding to 80–90 Ma) it is only 4 cm/yr. Speeds computed with CitcomS (Figure 8) are even smaller, reaching a maximum of only about 2.5 cm/yr with a semicircular plate of 33.7 degrees radius (plate area as 30–40 Ma) and dropping to 1 cm/yr. After comparing results of the first model with and without downhill forces, we expect that downhill forces not included in the second model can increase these values by about a factor 1.5–2. The smaller

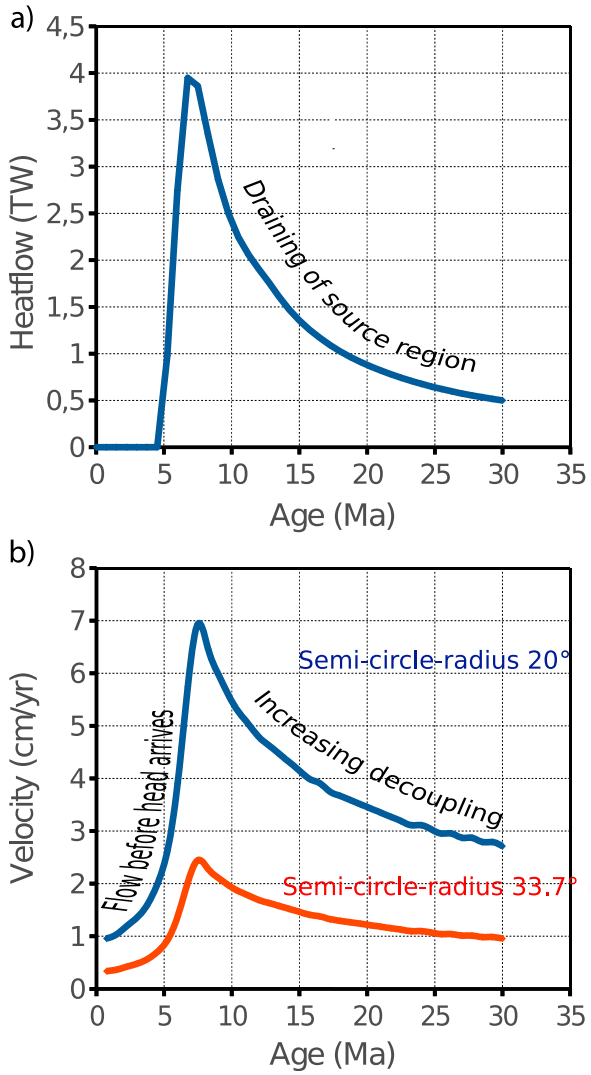

Figure 8. (a) Heat flux versus time for a plume computed with CitcomS. (b) Speed of "free" plate motion (tangential forces only) for the plume computed with CitcomS. The plate has the shape of a semicircular cap, with 33.7 degrees of arc radius (same area as the India plate 30–40 Ma, red line) or 20 degrees of arc radius (blue line); the plume impinges at the center of the straight plate boundary, thus transmitting the maximum torque.

values and drop in this case can be understood as caused by (1) the plume flux dropping more strongly, as explained above, and (2) reduced coupling of plate and underlying mantle, once the plume feeds into the asthenosphere and further reduces viscosity there. In the second model, the maximum in predicted plate speed and subsequent sharp drop occurring soon after the heat flux maximum reflects the very fast rising and spreading of the plume (within a few Myr at speeds of several tens of cm/yr) once it has reached the upper mantle. Only in the case of an even smaller plate (radius 20 degrees) resulting speeds are still appreciable.

[53] Second, we compute speeds with a realistic model of plate boundaries in 10 Myr intervals from *Torsvik et al.* [2010] (Figure 5). Computed speeds are lower here, because the plume is mostly either beneath the plate, in which case some compensation between forces occurs, or it is some distance away from the plate, and because of the different plate boundary geometry. For the Morondava/Marion plume, predicted plate speed drops as the plume moves away from the plate boundary (red continuous line in Figure 6b). The Deccan/Reunion plume (green continuous line), on the other hand, is overridden by the plate boundary after some time, and the maximum effect occurs at that time. For the Morondava/Marion plume, computed plate speed reaches values somewhat above 3 cm/yr between 60 and 90 Ma, whereas for the Deccan/Reunion plume it reaches between 5 and 6 cm/yr, between 40 and 30 Ma, corresponding to smaller plate area at that time. The combined effect (black line) is maximally about 7.5 cm/yr. For the Deccan/Reunion plume, the direction of predicted plate motion is typically ENE whereas the actual plate motion is more N to NNE. The difference can presumably be attributed to the fact that the plate only can move freely (relative to its neighboring plates) parallel to the transform faults and is blocked in the other directions. In Figure 6 we hence plot the projection of the "free" plate motion on to the direction N30E, roughly parallel to the transform faults. The 70 Ma plate geometry is used for 74–60 Ma, the 60 Ma geometry 64–50 Ma etc. hence the overlapping "steps" in the plot.

[54] The Indian lithosphere is thin with respect to other cratonic regions, and we have used its modern thickness in our computations. *Kumar et al.* [2007] suggested that this reduced thickness could be an effect of plume arrival, and it is possible that the thickness of the Indian lithosphere directly at the moment of plume arrival was much larger. If so, the Indian 'keel' into the mantle was deeper, and the coupling between the lithosphere and asthenosphere may have been stronger. We have run our models for different lithospheric thicknesses, from 150 to 400 km, and found that the increase in predicted plate speed due to greater lithosphere thickness is rather small and not qualitatively affecting our conclusions.

5. Discussion

[55] Our results indicate that the Morondava and Deccan plumes may each have contributed a few cm/yr to the velocity increase and decrease of the Indian plate. They cause a force on the plate in a similar direction as the force due to subduction, and therefore may cause an increase in plate speed of a few cm/yr. Our results show that a drop of plate speed following the initial increase does not necessarily require an increased resistance against plate motion but may simply reflect a drop in the driving force caused by the plume. Such a drop may be caused by (1) the plate moving away from the plume, (2) substantially reduced plume flux after initial eruption of the plume head, (3) reduced coupling between plate and mantle, if the plume causes a viscosity decrease in the asthenosphere. Comparison with observations indicates that the effect of plumes is by itself, in the case of Morondava perhaps, but in the case of Deccan almost certainly not, sufficient to explain the observed speedups and slowdowns of plate motion.

[56] The discrepancy is aggravated, as our estimate is probably rather an upper limit, because (1) computed plumes are rather "massive," at least in the model without

lateral viscosity variations, at the upper limit of what is compatible with seismic tomography; (2) other estimates indicate that the mass flux of plumes may be smaller than in our models; (3) for the plumes modeled here, computed dynamic topography is also rather large, compared to what is inferred from observations; and (4) computed plate speeds are for free plate motion; if the plate faces increased resistance elsewhere once it moves faster, the effect of plumes on plate motion will be reduced. With its short-lived maximum and subsequent decrease of plate speed, the CitcomS model appears to match the timing of observed plate speed variations qualitatively better, however this model predicts even lower plate speeds.

[57] Nevertheless, despite the obvious discrepancy in magnitude, the correspondence in timing remains intriguing: There is a short-lived maximum in plate speed after eruption of the Morondava LIP (Figure 3). We note, however, that the counterclockwise rotation of India (relative to Eurasia and Indo-Atlantic hot spots) during the 90–83.5 Ma interval occurs around a stage pole located close to the western India (Figure 2), resulting in a clear peak of the relative and absolute velocities for the eastern India only. Because the uncertainties for the 90 Ma rotations combined in our plate circuit model are unknown, it is not possible to test whether this peak in significant compared to the reconstruction error. Yet, the overall increase of the Indian plate velocity at ~90 Ma appears to be a robust feature in both relative and absolute kinematic models when compared to the lower velocities characteristic for the 120–90 Ma interval. The increase of plate speed following the Deccan plume around 66 Ma is perhaps somewhat longer and the maximum somewhat more delayed. This could indicate the effect of relative location of plume and plate boundary, where the maximum effect occurs as the plume is beneath, i.e., overridden by the plate boundary. Age data along the Reunion hot spot track indicate that the hot spot was located close to the Central Indian Ridge axis during ~58–49 Ma [*O'Neill et al.*, 2005]. We speculate that the discrepancy in magnitude could possibly be explained by a combination of the following:

[58] 1. Plume heads initially arrived beneath continental lithosphere, below which there was a less pronounced asthenosphere. Hence tangential forces were more efficiently transferred to the lithosphere than in our model. Subsequently, the opening of an ocean basin with a more pronounced asthenosphere reduced the coupling and caused a slowdown of the plate. Our calculations with a thicker lithosphere indicate that this is only a rather minor (~10%) effect.

[59] 2. There was some positive feedback mechanism.

[60] 3. The mechanism relating plumes and plate motion is more indirect than the one studied here. For example, the plume, rather than pushing the plate itself, weakens the asthenosphere, such that the attached slab can pull the plate faster. Such an indirect mechanism would also help to explain that the change of plate motion is not in the same direction as the computed push on the plate due to the plume. Such effects are not included in our models, and could be studied in future work. Nevertheless, aside from the relatively minor effects of the Deccan plume arrival below the Indian Plate, increased effectivity of slab pull due to decreased lithosphere-asthenosphere coupling seems to be the most logical candidate to explain the high India-Asia plate convergence rate around 55 Ma.

[61] The decrease in plate speed since ~50 Ma is hence to some extent probably due to a combination of reduced plume flux, reduced coupling with the plate and the plate moving away from the plume. However, these effects can only for a minor part explain the dramatic slowdown between 50 and 35 Ma. We speculate that a more pronounced slowdown could result, if, after the Deccan plume was no longer under the India plate, the above mentioned scenario was reversed, i.e., lithosphere-asthenosphere coupling was increased again and the effectivity of slab pull decreased. Again, this scenario could be modeled in future work.

[62] In the absence of such a quantitative model, a net decrease of slab pull forces as a result of continental subduction, in combination with increased resistivity at the subduction zone due to ongoing orogeny in the Himalayas and Tibet remains the most elegant explanation for the post-50 Ma slowdown.

[63] We can give an approximate estimate of the effect of increased topography as a result of collision on the plate convergence rates using the above-determined impedance: Additional topography h (in Tibet) causes additional pressure ρgh along the plate boundary, whereby ρ is (crustal) density and g is gravity. With a compensation depth d and a boundary length b we obtain a total force ρghdb. With a plate area A = lb, the force per plate area is ρghd/l. With ρ = 2700 kg/m^3, g = 10 m/s^2, d = 50 km, h = 5 km, and the extent of the plate in the direction orthogonal to the convergent boundary l = 6000 km we obtain a force per plate area of 1.125 MPa. With the impedance from above 2.067–2.775 MPa/(deg/Myr), and assuming that the entire modern topography of 5 km was created due to the 50 Ma collision, we arrive at the estimate that the additional topography in Tibet can cause a change (in this case, slowdown) of plate velocity by 0.41–0.54 deg/Myr or 4.5–6.1 cm/yr.

[64] It is likely, however, that Tibet was already an elevated region prior to 50 Ma as a result of major Cretaceous shortening of the Lhasa and Qiangtang terranes [*Kapp et al.*, 2005, 2007a]. Assuming ~20% crustal shortening of these terranes after 50 Ma (~15% for Lhasa [*Kapp et al.*, 2007b] and 25% for Qiangtang [*Kapp et al.*, 2005]), and using a modern crustal thickness of ~70 km [e.g., *Zhang et al.*, 2011] a Paleogene thickening of the Tibetan crust of ~14 km can be estimated, and an associated uplift of ~3 km during the India-Asia convergence rate slowdown assuming isostatic equilibrium, in line with the estimate based on palynology that Tibet was raised by ~2.5 km since the late Eocene [*Dupont-Nivet et al.*, 2008]. This would lead to a first-order estimate for the slowdown of about 2.7–3.6 cm/yr.

[65] A first-order estimate for reduction in slab pull due to subduction of continental lithosphere can be obtained in an analogous way, replacing ρh with $\Delta\rho$s whereby s = the length (or reduction of length for reduction of slab pull) of the slab pulling down, and $\Delta\rho$ is the (depth-averaged) density difference of the slab with respect to its surroundings. With estimated 2% relative density difference and a length of, e.g., 500–1000 km, slab pull can be several times larger than the collisional resistance. Hence, also decrease of slab pull can have a significant contribution to the observed slowdown. It is beyond the scope of this paper to calculate

the effects of continental collision and orogeny on the India-Asia convergence rate in detail, but these first-order estimates are clearly of the right magnitude. The general assumption that India-Asia convergence rate decrease since ~50 Ma results from collision seems therefore to be valid.

6. Summary and Conclusions

[66] A popular argument to assess the age of collision between India and Asia concerns the ~50 Ma onset of dramatic slowdown in the India-Asia convergence rate, from 16 cm/yr to ~5 cm/yr around 35 Ma. However, this argument does not take into account that between ~65 and 50 Ma an almost equally impressive acceleration of the India-Asia convergence rate occurred, following the extrusion of the Deccan LIP and the separation of India away from the Seychelles microcontinent. A similar speed-up episode, although of smaller magnitude, may be related to the emplacement of the Morondova LIP, and the separation between India and Madagascar. In this paper, we reassess the Indo-Atlantic plate circuit and confirm these fluctuations in relative India-Asia convergence rates.

[67] Using two different numerical models (one without and one with lateral viscosity variations) where the plume arrives exactly at the plate boundary, we assess whether plume head arrival and lateral sublithospheric flow induced by these can explain the convergence rate accelerations in the Indo-Asia convergence history. In addition, we test whether subsequent convergence rate decreases can be explained by the combined effect of decreased plume flux and motion of the Indian continent away from the plume.

[68] We conclude that plume head arrival may indeed increase the India-Asia convergence rate by several cm/yr, and that plume flux decrease and motion of India away from the plume may lead to a deceleration. The 90 Ma acceleration may perhaps entirely be explained by the effects of plume head arrival.

[69] The convergence rate increase following the arrival of the Deccan plume some 66 Ma ago from 8 to 16 cm/yr is much larger than can be explained by our modeling results. The large velocity increase may be best explained by increased ridge push–slab pull effects due to weakening of the lithosphere-asthenosphere boundary below the Indian continent, as postulated by *Kumar et al.* [2007]. Although part of the convergence rate decrease following 50 Ma may be attributed to plume flux decrease and motion of India away from the plume head, the bulk of convergence rate decrease is likely resulting from increased resistance at the convergent margin due to the Tibetan-Himalayan orogeny, decreased slab pull forces due to continental subduction, and perhaps the asthenosphere getting stronger again, as the plate moved away from the plume. Unless future work shows that this last effect alone is sufficient to explain the entire slowdown, the India-Asia convergence rate decrease starting around 50 Ma can hence be used as an argument to infer the arrival of Greater Indian continental lithosphere in a subduction zone around 55–50 Ma.

[70] **Acknowledgments.** D.J.J.vH. acknowledges Statoil for financial support (SPlates project). Trond Torsvik, Paul Kapp, Pete Lippert, Guillaume Dupont-Nivet, Pete DeCelles, Nadine McQuarrie, Colin Reeves, and Carmen Gaina are thanked for discussion. We acknowledge two anonymous reviewers for valuable comments.

References

Achache, J., V. Courtillot, and Y. X. Zhou (1984), Paleogeographic and tectonic evolution of southern Tibet since middle Cretaceous time: New paleomagnetic data and synthesis, *J. Geophys. Res.*, *89*, 10,311–10,339.

Agard, P., J. Omrani, L. Jolivet, and F. Mouthereau (2005), Convergence history across Zagros (Iran): Constraints from collisional and earlier deformation, *Int. J. Earth Sci.*, *94*, 401–419, doi:10.1007/s00531-005-0481-4.

Aitchison, J. C., J. R. Ali, and A. M. Davis (2007), When and where did India and Asia collide?, *J. Geophys. Res.*, *112*, B05423, doi:10.1029/2006JB004706.

Albers, M., and U. R. Christensen (1996), The excess temperature of plumes rising from the core-mantle boundary, *Geophys. Res. Lett.*, *23*, 3567–3570, doi:10.1029/96GL03311.

Ali, J. R., and J. C. Aitchison (2005), Greater India, *Earth Sci. Rev.*, *72*, 169–188, doi:10.1016/j.earscirev.2005.07.005.

Ali, J. R., and J. C. Aitchison (2006), Positioning Paleogene Eurasia problem: Solution for 60–50 Ma and broader tectonic implications, *Earth Planet. Sci. Lett.*, *251*, 148–155, doi:10.1016/j.epsl.2006.09.003.

Avouac, J.-P., P. Tapponnier, M. Bai, H. You, and G. Wang (1993), Active thrusting and folding along the northern Tien Shan and Late Cenozoic rotation of the Tarim relative to Dzungaria and Kazakhstan, *J. Geophys. Res.*, *98*, 6755–6804, doi:10.1029/92JB01963.

Bardintzeff, J.-M., J.-P. Liégois, B. Bonin, H. Bellon, and G. Rasamimanana (2010), Madagascar volcanic provinces linked to the Gondwana break-up: Geochemical and isotopic evidences for contrasting mantle sources, *Gondwana Res.*, *18*, 295–314, doi:10.1016/j.gr.2009.11.010.

Besse, J., and V. Courtillot (2002), Apparent and true polar wander and the geometry of the geomagnetic field over the last 200 Myr, *J. Geophys. Res.*, *107*(B11), 2300, doi:10.1029/2000JB000050.

Burke, K., and J. F. Dewey (1973), Plume-generated triple junctions: Key indicators in applying plate tectonics to old rocks, *J. Geol.*, *81*, 406–433, doi:10.1086/627882.

Cai, J.-X., and K.-J. Zhang (2009), A new model for the Indochina and South China collision during the Late Permian to the Middle Triassic, *Tectonophysics*, *467*, 35–43, doi:10.1016/j.tecto.2008.12.003.

Cande, S. C., and D. V. Kent (1995), Revised calibration of the geomagnetic polarity timescale for the Late Cretaceaous and Cenozoic, *J. Geophys. Res.*, *100*, 6093–6095, doi:10.1029/94JB03098.

Cande, S. C., P. Patriat, and J. Dyment (2010), Motion between the Indian, Antarctic and African plates in the early Cenozoic, *Geophys. J. Int.*, *183*, 127–149, doi:10.1111/j.1365-246X.2010.04737.x.

Chang, T. (1988), Estimating the relative rotation of two tectonic plates from boundary crossings, *J. Am. Stratigr. Assoc.*, *83*, 1178–1183, doi:10.2307/2290152.

Chang, T., J. M. Stock, and P. Molnar (1990), The rotation group in plate tectonics and the representation of uncertainties in plate reconstructions, *Geophys. J. Int.*, *101*, 649–661.

Chen, J., B. Huang, and L. Sun (2010), New constraints to the onset of the India–Asia collision: Paleomagnetic reconnaissance on the Linzizong Group in the Lhasa Block, China, *Tectonophysics*, *489*, 189–209.

Collier, J. S., V. Sansom, O. Ishikuza, R. N. Taylor, T. A. Minshull, and R. B. Whitmarsh (2008), Age of Seychelles–India break-up, *Earth Planet. Sci. Lett.*, *272*, 264–277, doi:10.1016/j.epsl.2008.04.045.

Copley, A., J.-P. Avouac, and J.-Y. Royer (2010), The India-Asia collision and the Cenozoic slowdown of the Indian plate; implications for the forces, *J. Geophys. Res.*, *115*, B03410, doi:10.1029/2009JB006634.

Corfield, R. I., M. P. Searle, and R. B. Pederson (2001), Tectonic setting, origin, and obduction history of the spontang ophiolite, Ladakh Himalaya, NW India, *J. Geol.*, *109*, 715–736, doi:10.1086/323191.

Courtillot, V., C. Jaupart, I. Manighetti, P. Tapponnier, and J. Besse (1999), On causal links between flood basalts and continental breakup, *Earth Planet. Sci. Lett.*, *166*, 177–195, doi:10.1016/S0012-821X(98)00282-9.

Cowgill, E. (2010), Cenozoic right-slip faulting along the eastern margin of the Pamir salient, northwestern China, *Geol. Soc. Am. Bull.*, *122*, 145–161, doi:10.1130/B26520.1.

Cowgill, E., A. Yin, T. M. Harrison, and X.-F. Wang (2003), Reconstruction of the Altyn Tagh fault based on U-Pb geochronology: Role of back thrusts, mantle sutures, and heterogeneous crustal strength in forming the Tibetan Plateau, *J. Geophys. Res.*, *108*(B7), 2346, doi:10.1029/2002JB002080.

Cunningham, W. D. (2005), Active intracontinental transpressional mountain building in the Mongolian Altai: Defining a new class of orogen, *Earth Planet. Sci. Lett.*, *240*, 436–444, doi:10.1016/j.epsl.2005.09.013.

Davies, G. (1988), Ocean bathymetry and mantle convection: 1. Large-scale flows and hotspots, *J. Geophys. Res.*, *93*, 10,467–10,480, doi:10.1029/JB093iB09p10467.

DeCelles, P. G., D. M. Robinson, and G. Zandt (2002), Implications of shortening in the Himalayan fold-thrust belt for uplift of the Tibetan Plateau, *Tectonics*, *21*(6), 1062, doi:10.1029/2001TC001322.

DeMets, C., R. G. Gordon, and J.-Y. Royer (2005), Motion between the Indian, Capricorn and Somalian plates since 20 Ma: Implications for the timing and magnitude of distributed lithospheric deformation in the equatorial Indian ocean, *Geophys. J. Int.*, *161*, 445–468, doi:10.1111/j.1365-246X.2005.02598.x.

Dewey, J. F., R. M. Shackleton, C. Chang, and Y. Sun (1988), The tectonic evolution of the Tibetan Plateau, *Philos. Trans. R. Soc. London, A*, *327*, 379–413, doi:10.1098/rsta.1988.0135.

Ding, L., P. Kapp, and X. Wan (2005), Paleocene–Eocene record of ophiolite obduction and initial India-Asia collision, south central Tibet, *Tectonics*, *24*, TC3001, doi:10.1029/2004TC001729.

Doubrovine, P. V., and J. A. Tarduno (2008), Linking the Late Cretaceous to Paleogene Pacific plate and the Atlantic bordering continents using plate circuits and paleomagnetic data, *J. Geophys. Res.*, *113*, B07104, doi:10.1029/2008JB005584.

Dupont-Nivet, G., W. Krijgsman, C. G. Langereis, H. A. Abels, S. Dai, and X. Fang (2007), Tibetan plateau aridification linked to global cooling at the Eocene-Oligocene transition, *Nature*, *445*, 635–638, doi:10.1038/nature05516.

Dupont-Nivet, G., C. Hoorn, and M. Konert (2008), Tibetan uplift prior to the Eocene-Oligocene climate transition: Evidence from pollen analysis of the Xining Basin, *Geology*, *36*, 987–990, doi:10.1130/G25063A.1.

Dupont-Nivet, G., P. Lippert, D. J. J. van Hinsbergen, M. J. M. Meijers, and P. Kapp (2010a), Paleolatitude and age of the Indo-Asia collision: Paleomagnetic constraints, *Geophys. J. Int.*, *182*, 1189–1198, doi:10.1111/j.1365-246X.2010.04697.x.

Dupont-Nivet, G., D. J. J. van Hinsbergen, and T. H. Torsvik (2010b), Persistently shallow paleomagnetic inclinations in Asia: Tectonic implications for the Indo-Asia collision, *Tectonics*, *29*, TC5016, doi:10.1029/2008TC002437.

Dziewonski, A. M., and D. L. Anderson (1981), Preliminary reference Earth model, *Phys. Earth Planet. Inter.*, *25*, 297–356, doi:10.1016/0031-9201(81)90046-7.

Eagles, G., and M. Konig (2008), A model of plate kinematics in Gondwana breakup, *Geophys. J. Int.*, *173*, 703–717, doi:10.1111/j.1365-246X.2008.03753.x.

Farnetani, C. G., and H. Samuel (2005), Beyond the thermal plume paradigm, *Geophys. Res. Lett.*, *32*, L07311, doi:10.1029/2005GL022360.

Gaina, C., W. R. Roest, and R. D. Muller (2002), Late Cretaceous-Cenozoic deformation of northeast Asia, *Earth Planet. Sci. Lett.*, *197*, 273–286, doi:10.1016/S0012-821X(02)00499-5.

Gaina, C., R. D. Muller, B. Brown, and T. Ishihara (2003), Microcontinent formation around Australia, in *Evolution and Dynamics of the Australian Plate*, edited by R. R. Hills and R. D. Muller, *Spec. Pap. Geol. Soc. Am.*, *372*, 405–416.

Gaina, C., R. D. Muller, B. Brown, T. Ishihara, and S. Ivanov (2007), Breakup and early seafloor spreading between India and Antarctica, *Geophys. J. Int.*, *170*, 151–169, doi:10.1111/j.1365-246X.2007.03450.x.

Ganerød, M., T. H. Torsvik, D. J. J. van Hinsbergen, F. Corfu, C. Gaina, S. Werner, T. Owen-Smith, L. Ashwal, S. Webb, and B. W. H. Hendriks (2011), Paleoposition of the Seychelles continent in relation to the Decan Traps and the Plume Generation Zone in KT boundary time, in *The Formation and Evolution of Africa: A Synopsis of 3.8 Ga of Earth History*, edited by D. J. J. van Hinsbergen et al., *Geol. Soc. Spec. Publ.*, *357*, in press.

Gnos, E., A. Immanhauser, and T. Peters (1997), Late Cretaceous/early Tertiary convergence between the Indian and Arabian plates recorded in ophiolites and related sediments, *Tectonophysics*, *271*, 1–19, doi:10.1016/S0040-1951(96)00249-1.

Gradstein, F. M., F. P. Agterberg, J. G. Ogg, J. S. Hardenbol, P. van Veen, J. Thierry, and Z. H. Huang (1994), A Mesozoic timescale, *J. Geophys. Res.*, *99*, 24,051–24,074, doi:10.1029/94JB01889.

Gradstein, F. M., J. G. Ogg, and A. G. Smith (2004), *A Geologic Time Scale 2004*, Cambridge Univ. Press, Cambridge, U. K.

Green, O. R., M. P. Searle, R. I. Corfield, and R. M. Corfield (2008), Cretaceous-Tertiary carbonate platform evolution and the age of the India-Asia collision along the Ladakh Himalaya (Northwest India), *J. Geol.*, *116*, 331–353, doi:10.1086/588831.

Guillot, S., E. Garzanti, D. Baratoux, D. Marquer, G. Mahéo, and J. de Sigoyer (2003), Reconstructing the total shortening history of the NW Himalaya, *Geochem. Geophys. Geosyst.*, *4*(7), 1064, doi:10.1029/2002GC000484.

Guillot, S., G. Maheo, J. de Sigoyer, K. H. Hattori, and A. Pecher (2008), Tethyan and Indian subduction viewed from the Himalayan high- to ultrahigh-pressure metamorphic rocks, *Tectonophysics*, *451*, 225–241, doi:10.1016/j.tecto.2007.11.059.

Guilmette, C., R. Hébert, C. Wang, and M. Villeneuve (2009), Geochemistry and geochronology of the metamorphic sole underlying the Xigaze Ophiolite, Yarlung Zangbo Suture Zone, South Tibet, *Lithos*, *112*, 149–162, doi:10.1016/j.lithos.2009.05.027.

Gurnis, M., and T. H. Torsvik (1994), Rapid drift of large continents during the late Precambrian and Paleozoic: Paleomagnetic constraints and dynamic models, *Geology*, *22*, 1023–1026, doi:10.1130/0091-7613(1994)022<1023:RDOLCD>2.3.CO;2.

Hafkenscheid, E., M. J. R. Wortel, and W. Spakman (2006), Subduction history of the Tethyan region derived from seismic tomography and tectonic reconstructions, *J. Geophys. Res.*, *111*, B08401, doi:10.1029/2005JB003791.

Hager, B., and R. O'Connell (1981), A simple global model of plate dynamics and mantle convection, *J. Geophys. Res.*, *86*, 4843–4867, doi:10.1029/JB086iB06p04843.

Hall, R., M. W. A. van Hattum, and W. Spakman (2008), Impact of India-Asia collision on SE Asia: The record in Borneo, *Tectonophysics*, *451*, 366–389, doi:10.1016/j.tecto.2007.11.058.

Hill, R. I. (1991), Starting plumes and continental break-up, *Earth Planet. Sci. Lett.*, *104*, 398–416, doi:10.1016/0012-821X(91)90218-7.

Hofmann, C., G. Feraud, and V. Courtillot (2000), $^{40}Ar/^{39}Ar$ dating of mineral separates and whole rocks from the Western Ghats lava pile: Further constraints on duration and age of the Deccan traps, *Earth Planet. Sci. Lett.*, *180*, 13–27, doi:10.1016/S0012-821X(00)00159-X.

Horner-Johnson, B. C., R. G. Gordon, and D. F. Argus (2007), Plate kinematic evidence for the existence of a distinct plate between the Nubian and Somalian plates along the Southwest Indian Ridge, *J. Geophys. Res.*, *112*, B05418, doi:10.1029/2006JB004519.

Hsü, K. J., G.-T. Pan, and A. M. C. Sengör (1995), Tectonic evolution of the Tibetan Plateau: A working hypothesis based on the archipelago model of orogenesis, *Int. Geol. Rev.*, *37*, 473–508, doi:10.1080/00206819509465414.

Ji, W.-Q., F.-Y. Wu, S.-L. Chung, J.-X. Li, and C.-Z. Liu (2009), Zircon U–Pb geochronology and Hf isotopic constraints on petrogenesis of the Gangdese batholith, southern Tibet, *Chem. Geol.*, *262*, 229–245, doi:10.1016/j.chemgeo.2009.01.020.

Johnson, M. R. W. (2002), Shortening budgets and the role of continental subduction during the India-Asia collision, *Earth Sci. Rev.*, *59*, 101–123, doi:10.1016/S0012-8252(02)00071-5.

Jourdan, F., G. Feraud, H. Bertrand, and M. K. Watkeys (2007), From flood basalts to the inception of oceanization: Example from the 40Ar/39Ar high-resolution picture of the Karoo large igneous province, *Geochem. Geophys. Geosyst.*, *8*, Q02002, doi:10.1029/2006GC001392.

Kapp, P., and J. H. Guynn (2004), Indian punch rifts Tibet, *Geology*, *32*, 993–996, doi:10.1130/G20689.1.

Kapp, P. A., A. Yin, C. E. Manning, M. A. Murphy, T. M. Harrison, M. Spurlin, L. Ding, D. Xi-Guang, and W. Cun-Ming (2000), Blueschist-bearing metamorphic core complexes in the Qiangtang block reveal deep crustal structure of northern Tibet, *Geology*, *28*, 19–22, doi:10.1130/0091-7613(2000)28<19:BMCCIT>2.0.CO;2.

Kapp, P., A. Yin, T. M. Harrison, and L. Ding (2005), Cretaceous-Tertiary shortening, basin development and volcanism in central Tibet, *Geol. Soc. Am. Bull.*, *117*, 865–878, doi:10.1130/B25595.1.

Kapp, P., P. G. DeCelles, G. E. Gehrels, M. Heizler, and L. Ding (2007a), Geological records of the Cretaceous Lhasa-Qiangtang and Indo-Asian collisions in the Nima basin area, central Tibet, *Geol. Soc. Am. Bull.*, *119*, 917–933, doi:10.1130/B26033.1.

Kapp, P., P. G. DeCelles, A. L. Leier, J. M. Fabijanic, S. He, A. Pullen, G. E. Gehrels, and L. Ding (2007b), The Gangdese retroarc thrust belt revealed, *GSA Today*, *17*, 4–9, doi:10.1130/GSAT01707A.1.

Klitgord, K. D., and H. Schouten (1986), Plate kinematics of the central Atlantic, in *The Western North Atlantic Region*, *Geol. North Am.*, vol. M, edited by P. R. Vogt and B. E. Tucholke, pp. 351–378, Geol. Soc. Am., Boulder, Colo.

Klootwijk, C. T. (1984), A review of Indian Phanerozoic palaeomagnetism: Implications for the India-Asia collision, *Tectonophysics*, *105*, 331–353, doi:10.1016/0040-1951(84)90212-9.

Kumar, P., X. Yuan, M. R. Kumar, R. Kind, X. Li, and R. K. Chadha (2007), The rapid drift of the Indian tectonic plate, *Nature*, *449*, 894–897, doi:10.1038/nature06214.

Lacassin, R., et al. (2004), Large-scale geometry, offset and kinematic evolution of the Karakorum fault, Tibet, *Earth Planet. Sci. Lett.*, *219*, 255–269, doi:10.1016/S0012-821X(04)00006-8.

Lee, T.-Y., and L. A. Lawver (1995), Cenozoic plate reconstruction of Southeast Asia, *Tectonophysics*, *251*, 85–138, doi:10.1016/0040-1951(95)00023-2.

Leech, M. L., S. C. Singh, A. K. Jain, S. L. Klemperer, and R. M. Manickavasagam (2005), The onset of India–Asia continental collision: Early, steep subduction required by the timing of UHP metamorphism in

the western Himalaya, *Earth Planet. Sci. Lett.*, *234*, 83–97, doi:10.1016/j.epsl.2005.02.038.

Leloup, P. H., R. Lacassin, P. Tapponnier, U. Schärer, Z. Dalai, L. Xiaohan, Z. Liangshang, J. Shaocheng, and T. T. Phan Trong (1995), The Ailao Shan-Red River shear zone (Yunnan, China), Tertiary transform boundary of Indochina, *Tectonophysics*, *251*, 3–84, doi:10.1016/0040-1951(95)00070-4.

Lemaux, J. R., R. G. Gordon, and J.-Y. Royer (2002), Location of the Nubia-Somalia boundary along the Southwest Indian Ridge, *Geology*, *30*, 339–342, doi:10.1130/0091-7613(2002)030<0339:LOTNSB>2.0.CO;2.

Liebke, U., E. Appel, U. Neumann, B. Antolin, L. Ding, and X. Qiang (2010), Position of the Lhasa terrane prior to India-Asia collision derived from palaeomagnetic inclinations of 53 Ma old dykes of the Linzhou Basin: Constraints on the age of collision and post-collisional shortening within the Tibetan Plateau, *Geophys. J. Int.*, *182*, 1199–1215, doi:10.1111/j.1365-246X.2010.04698.x.

Lippert, P. C., D. J. J. van Hinsbergen, G. Dupont-Nivet, and P. Kapp (2010), Consensus on the Eocene latitude of Lhasa and the age of the Tethyan Himalaya-Asia collision?, Abstract T33F–03 presented at 2010 Fall Meeting, AGU, San Francisco, Calif., 13–17 Dec.

Long, S. P., N. McQuarrie, T. Tobgay, and D. Grujic (2011), Geometry and crustal shortening of the Himalayan fold-thrust belt, eastern and central Bhutan, *Geol. Soc. Am. Bull.*, doi:10.1130/B30203.1, in press.

McQuarrie, N., J. M. Stock, C. Verdel, and B. Wernicke (2003), Cenozoic evolution of the Neotethys and implications for the causes of plate motions, *Geophys. Res. Lett.*, *30*(20), 2036, doi:10.1029/2003GL017992.

Merkouriev, S., and C. DeMets (2008), A high-resolution model for Eurasia-North America plate kinematics since 20 Ma, *Geophys. J. Int.*, *173*, 1064–1083, doi:10.1111/j.1365-246X.2008.03761.x.

Molnar, P., and T. Atwater (1973), Relative motion of hot spots in the mantle, *Nature*, *246*, 288–291, doi:10.1038/246288a0.

Molnar, P., and J. M. Stock (1985), A method for bounding uncertainties in combined plate reconstructions, *J. Geophys. Res.*, *90*, 12,537–12,544, doi:10.1029/JB090iB14p12537.

Molnar, P., and J. M. Stock (2009), Slowing of India's convergence with Eurasia since 20 Ma and its implications for Tibetan mantle dynamics, *Tectonics*, *28*, TC3001, doi:10.1029/2008TC002271.

Molnar, P., and P. Tapponnier (1975), Cenozoic tectonics of Asia: Effects of a continental collision, *Science*, *189*, 419–426, doi:10.1126/science.189.4201.419.

Molnar, P., F. Pardo-Casas, and J. M. Stock (1988), The Cenozoic and Late Cretaceous evolution of the Indian Ocean basin: Uncertainties in the reconstructed positions of the Indian, African, and Antarctic plates, *Basin Res.*, *1*, 23–40, doi:10.1111/j.1365-2117.1988.tb00003.x.

Müller, R. D., J.-Y. Royer, S. C. Cande, W. R. Roest, and S. Maschenkov (1999), New constraints on the Late Cretaceous-Tertiary plate tectonic evolution of the Caribbean, in *Caribbean Basins*, vol. 4, *Sedimentary Basins of the World: Amsterdam*, edited by P. Mann, pp. 33–57, Elsevier, New York.

Najman, Y. (2006), The detrital record of orogenesis: A review of approaches and techniques used in the Himalayan sedimentary basins, *Earth Sci. Rev.*, *74*, 1–72.

Najman, Y., and E. Garzanti (2000), Reconstructing early Himalayan tectonic evolution and paleogeography from Tertiary foreland basin sedimentary rocks, northern India, *Geol. Soc. Am. Bull.*, *112*, 435–449, doi:10.1130/0016-7606(2000)112<435:REHTEA>2.0.CO;2.

Najman, Y., A. Carter, G. Oliver, and E. Garzanti (2005), Provenance of Eocene foreland basin sediments, Nepal: Constraints to the timing and diachroneity of early Himalayan orogenesis, *Geology*, *33*, 309–312, doi:10.1130/G21161.1.

Najman, Y., et al. (2010), The timing of India-Asia collision: Geological, biostratigraphic and palaeomagnetic constraints, *J. Geophys. Res.*, *115*, B12416, doi:10.1029/2010JB007673.

Nolet, G., S.-i. Karato, and R. Montelli (2006), Plume fluxes from seismic tomography, *Earth Planet. Sci. Lett.*, *248*, 685–699, doi:10.1016/j.epsl.2006.06.011.

O'Neill, C., D. Muller, and B. Steinberger (2005), On the uncertainties in hot spot reconstructions and the significance of moving hot spot reference frames, *Geochem. Geophys. Geosyst.*, *6*, Q04003, doi:10.1029/2004GC000784.

Patriat, P., and J. Achache (1984), India-Asia collision chronology and its implications for crustal shortening and driving mechanisms, *Nature*, *311*, 615–621, doi:10.1038/311615a0.

Patzelt, A., H. Li, J. Wang, and E. Appel (1996), Palaeomagnetism of Cretaceous to Tertiary sediments from southern Tibet: Evidence for the extent of the northern margin of India prior to the collision with Eurasia, *Tectonophysics*, *259*, 259–284, doi:10.1016/0040-1951(95)00181-6.

Pedersen, R. B., M. P. Searle, A. Carter, and P. C. Bandopadhyay (2010), U–Pb zircon age of the Andaman ophiolite: Implications for the beginning of subduction beneath the Andaman–Sumatra arc, *J. Geol. Soc.*, *167*, 1105–1112, doi:10.1144/0016-76492009-151.

Peltzer, G., and P. Tapponnier (1988), Formation and evolution of strike-slip faults, rifts and basins during the India-Adia collision: An experimental approach, *J. Geophys. Res.*, *93*, 15,085–15,177.

Press, W. H., B. P. Flannery, S. A. Teukolski, and W. T. Vetterling (1986), *Numerical Recipes: The Art of Scientific Computing*, 1256 pp., Cambridge Univ. Press, Cambridge, U. K.

Putirka, K. D. (2005), Mantle potential temperatures at Hawaii, Iceland and the mid-ocean ridge system, as inferred from olivine phenocrysts: Evidence for thermally driven mantle plumes, *Geochem. Geophys. Geosyst.*, *6*, Q05L08, doi:10.1029/2005GC000915.

Replumaz, A., and P. Tapponnier (2003), Reconstruction of the deformed collision zone Between India and Asia by backward motion of lithospheric blocks, *J. Geophys. Res.*, *108*(B6), 2285, doi:10.1029/2001JB000661.

Ricard, Y., and C. Vigny (1989), Mantle dynamics with induced plate tectonics, *J. Geophys. Res.*, *94*, 17,543–17,559, doi:10.1029/JB094iB12p17543.

Robinson, A. C. (2009), Geologic offsets across the northern Karakorum fault: Implications for its role and terrane correlations in the western Himalayan-Tibetan orogen, *Earth Planet. Sci. Lett.*, *279*, 123–130, doi:10.1016/j.epsl.2008.12.039.

Rowley, D. B. (1996), Age of initiation of collision between India and Asia: A review of stratigraphic data, *Earth Planet. Sci. Lett.*, *145*, 1–13, doi:10.1016/S0012-821X(96)00201-4.

Royden, L. H., B. C. Burchfiel, and R. D. Van der Hilst (2008), The geological evolution of the Tibetan Plateau, *Science*, *321*, 1054–1058, doi:10.1126/science.1155371.

Ruedas, T., H. Schmeling, G. Marquart, A. Kreutzmann, and A. Junge (2004), Temperature and melting of a ridge-centered plume with application to Iceland, part I: Dynamics and crust production, *Geophys. J. Int.*, *158*, 729–743, doi:10.1111/j.1365-246X.2004.02311.x.

Schettino, A., and C. R. Scotese (2005), Apparent polar wander paths for the major continents (200 Ma to the present day): A palaeomagnetic reference frame for global tectonic reconstructions, *Geophys. J. Int.*, *163*, 727–759, doi:10.1111/j.1365-246X.2005.02638.x.

Schubert, G., D. L. Turcotte, and P. Olson (2001), *Mantle Convection in the Earth and Planets*, Cambridge Univ. Press, New York, doi:10.1017/CBO9780511612879.

Schwab, M., et al. (2004), Assembly of the Pamirs: Age and origin of magmatic belts from the southern Tien Shan to the southern Pamirs and their relation to Tibet, *Tectonics*, *23*, TC4002, doi:10.1029/2003TC001583.

Searle, M. P. (2006), Role of the Red River sear zone, Yunnan and Vietnam, in the continental extrusion of SE Asia, *J. Geol. Soc.*, *163*, 1025–1036.

Searle, M. P., and R. J. Phillips (2007), Relationships between right-lateral shear along the Karakoram fault and metamorphism, magmatism, exhumation and uplift: Evidence from the K2–Gasherbrum–Pangong ranges, north Pakistan and Ladakh, *J. Geol. Soc.*, *164*, 439–450, doi:10.1144/0016-76492006-072.

Searle, M. P., and P. J. Treloar (2010), Was Late Cretaceous - Palaeocene obduction of ophiolite complexes the primary cause of crustal thickening and regional metamorphism in the Pakistan Himalaya?, *Geol. Soc. Spec. Publ.*, *338*, 345–359.

Sleep, N. (1990), Hotspots and mantle plumes: Some phenomenology, *J. Geophys. Res.*, *95*, 6715–6736, doi:10.1029/JB095iB05p06715.

Spurlin, M. S., A. Yin, B. K. Horton, J. Zhou, and J. Wang (2005), Structural evolution of the Yushu-Nangqian region and its relationship to syncollisional igneous activity, east-central Tibet, *Geol. Soc. Am. Bull.*, *117*, 1293–1317, doi:10.1130/B25572.1.

Srivastava, S. P., and W. R. Roest (1989), Sea floor spreading history II–IV, in *East Coast Basin Atlas Series: Labrador Sea*, edited by J. C. Bell, pp. 100–109, Atl. Geosci. Cent., Geol. Surv. of Can., Dartmouth, Nova Scotia.

Srivastava, S. P., and C. R. Tapscott (1986), Plate kinematics of the North Atlantic, in *The Western North Atlantic Region*, *Geol. North Am.*, vol. M, edited by P. R. Vogt and B. E. Tucholke, pp. 379–404, Geol. Soc. of Am., Boulder, Colo.

Srivastava, S. P., H. Schouten, W. R. Roest, K. D. Klitgord, L. C. Kovacs, J. Verhoef, and R. Macnab (1990), Iberian plate kinematics: A jumping plate boundary between Eurasia and Africa, *Nature*, *344*, 756–759, doi:10.1038/344756a0.

Steinberger, B., and A. Calderwood (2006), Models of large-scale viscous flow in the Earth's mantle with constraints from mineral physics and surface observations, *Geophys. J. Int.*, *167*, 1461–1481, doi:10.1111/j.1365-246X.2006.03131.x.

Steinberger, B., H. Schmeling, and G. Marquart (2001), Large-scale lithospheric stress field and topography induced by global mantle circulation, *Earth Planet. Sci. Lett.*, *186*, 75–91, doi:10.1016/S0012-821X(01)00229-1.

Stock, J. M., and P. Molnar (1983), Some geometrical aspects of uncertainties in combined plate reconstructions, *Geology*, *11*, 697–701, doi:10.1130/0091-7613(1983)11<697:SGAOUI>2.0.CO;2.

Stock, J. M., P. Molnar, and T. Chang (1990), The rotation group in plate tectonics and the representation of uncertainties in plate reconstructions, *Geophys. J. Int.*, *101*, 649–661, doi:10.1111/j.1365-246X.1990.tb05576.x.

Sun, Z., W. Jiang, H. Li, J. L. Pei, and Z. Zhu (2010), New paleomagnetic results of Paleocene volcanic rocks from the Lhasa block: Tectonic implications for the collision of India and Asia, *Tectonophysics*, *490*, 257–266.

Tan, E., E. Choi, P. Thoutireddy, M. Gurnis, and M. Aivazis (2006), Geoframework: Coupling multiple modes of mantle convection within a computational framework, *Geochem. Geophys. Geosyst.*, *7*, Q06001, doi:10.1029/2005GC001155.

Tan, X., S. Gilder, K. P. Kodama, W. Jiang, Y. Han, H. Zhang, H. Xu, and D. Zhou (2010), New paleomagnetic results from the Lhasa block: Revised estimation of latitudinal shortening across Tibet and implications for dating the India–Asia collision, *Earth Planet. Sci. Lett.*, *293*, 396–404.

Taylor, M., A. Yin, F. J. Ryerson, P. Kapp, and L. Ding (2003), Conjugate strike-slip faulting along the Bangong-Nujiang suture zone accommodates coeval east-west extension and north-south shortening in the interior of the Tibetan Plateau, *Tectonics*, *22*(4), 1044, doi:10.1029/2002TC001361.

Torsvik, T. H., R. D. Tucker, L. D. Ashwal, E. A. Eide, N. A. Rakotosolofo, and M. J. De Wit (1998), Late Cretaceous magmatism in Madagascar: Palaeomagnetic evidence for a stationary Marion hotspot, *Earth Planet. Sci. Lett.*, *164*, 221–232, doi:10.1016/S0012-821X(98)00206-4.

Torsvik, T. H., R. D. Tucker, L. D. Ashwal, L. M. Carter, B. Jamtveit, K. T. Vidyadharan, and P. Venkataramana (2000), Late Cretaceous India-Madagascar fit and timing of break-up related magmatism, *Terra Nova*, *12*, 220–224, doi:10.1046/j.1365-3121.2000.00300.x.

Torsvik, T. H., R. van der Voo, J. G. Meert, J. Mosar, and H. J. Walderhaug (2001), Reconstructions of the continents around the North Atlantic at about the 60th parallel, *Earth Planet. Sci. Lett.*, *187*, 55–69, doi:10.1016/S0012-821X(01)00284-9.

Torsvik, T. H., M. A. Smethurst, K. Burke, and B. Steinberger (2006), Large igneous provinces generated from the margins of the large low-velocity provinces in the deep mantle, *Geophys. J. Int.*, *167*, 1447–1460, doi:10.1111/j.1365-246X.2006.03158.x.

Torsvik, T. H., R. D. Müller, R. Van der Voo, B. Steinberger, and C. Gaina (2008), Global plate motion frames: Toward a unified model, *Rev. Geophys.*, *46*, RG3004, doi:10.1029/2007RG000227.

Torsvik, T. H., B. Steinberger, M. Gurnis, and C. Gaina (2010), Plate tectonics and net lithosphere rotation over the past 150 My, *Earth Planet. Sci. Lett.*, *291*, 106–112, doi:10.1016/j.epsl.2009.12.055.

Valli, F., N. Arnaud, P. H. Leloup, E. R. Sorel, G. Mahéo, R. Lacassin, S. Guillot, H. Li, P. Tapponnier, and Z. Xu (2007), Twenty million years of continuous deformation along the Karakorum fault, western Tibet: A thermochronological analysis, *Tectonics*, *26*, TC4004, doi:10.1029/2005TC001913.

van der Meer, D. G., W. Spakman, D. J. J. van Hinsbergen, M. L. Amaru, and T. H. Torsvik (2010), Toward absolute plate motions constrained by lower mantle slab remnants, *Nat. Geosci.*, *3*, 36–40, doi:10.1038/ngeo708.

Wang, C. S., X. H. Li, X. M. Hu, and L. F. Jansa (2002), Latest marine horizon north of Qomolangma (Mt Everest): Implications for closure Tethys seaway and collision tectonics, *Terra Nova*, *14*, 114–120, doi:10.1046/j.1365-3121.2002.00399.x.

White, R., and D. McKenzie (1989), Magmatism at rift zones: The generation of volcanic continental margins and flood basalts, *J. Geophys. Res.*, *94*, 7685–7729, doi:10.1029/JB094iB06p07685.

Yin, A., and T. M. Harrison (2000), Geologic evolution of the Himalayan-Tibetan orogen, *Annu. Rev. Earth Planet. Sci.*, *28*, 211–280, doi:10.1146/annurev.earth.28.1.211.

Yin, A., S. Nie, P. Craig, T. M. Harrison, F. J. Ryerson, Q. Xianglin, and Y. Geng (1998), Late Cenozoic tectonic evolution of the southern Chinese Tian Shan, *Tectonics*, *17*, 1–27, doi:10.1029/97TC03140.

Yue, Y., S. A. Graham, B. D. Ritts, and J. L. Wooden (2005), Detrital zircon provenance evidence for large-scale extrusion along the Altyn Tagh fault, *Tectonophysics*, *406*, 165–178, doi:10.1016/j.tecto.2005.05.023.

Zhang, Z., L. Yang, J. Teng, and J. Badal (2011), An overview of the earth crust under China, *Earth Sci. Rev.*, *104*, 143–166, doi:10.1016/j.earscirev.2010.10.003.

Zhong, S., M. T. Zuber, L. N. Moresi, and M. Gurnis (2000), The role of temperature-dependent viscosity and surface plates in spherical shell models of mantle convection, *J. Geophys. Res.*, *105*, 11,063–11,082, doi:10.1029/2000JB900003.

Zhu, B., W. S. F. Kidd, D. B. Rowley, B. S. Currie, and N. Shafique (2005), Age of initiation of the India-Asia collision in the east-central Himalaya, *J. Geol.*, *113*, 265–285, doi:10.1086/428805.

P. V. Doubrovine and D. J. J. van Hinsbergen, Physics of Geological Processes, University of Oslo, Sem Sælands vei 24, N-0316 Oslo, Norway. (d.v.hinsbergen@fys.uio.no)

R. Gassmöller, Institute for Geosciences, Friedrich Schiller University, Burgweg 11, D-07749 Jena, Germany.

B. Steinberger, Helmholtz Centre Potsdam, German Research Centre for Geosciences, Telegrafenberg, D-14473 Potsdam, Germany.